

VISVESVARAYA TECHNOLOGICAL UNIVERSITY  
JNANA SANGAMA, BELAGAVI – 590014



**A DISSERTATION REPORT ON**

**“Measurement of Laminar Flame Speed of LPG-Air Mixtures with  
Cylindrical Flame Tube Method”**

**SUBMITTED BY:**

**Mr. ABHINANDAN D. KADAM**

**[USN: 2JI16ME002]**

**Mr. ANUP J. GOURGONDA**

**[USN: 2JI16ME703]**

**Mr. NIKHIL P. DAPHALE**

**[USN: 2JI16ME026]**

**Mr. SAJAN V. ASNOTIKAR**

**[USN: 2JI16ME012]**

Under the Guidance of

**Dr. M. Sreedhar Babu**

Associate Professor, Department of Mechanical Engineering,  
Jain College of Engineering, Belagavi



**DEPARTMENT OF MECHANICAL ENGINEERING  
JAIN COLLEGE OF ENGINEERING, BELAGAVI  
2019-2020**

Sri Bhagawan Mahaveer Jain Educational and Cultural Trust's

# **JAIN COLLEGE OF ENGINEERING, BELAGAVI**

DEPARTMENT OF MECHANICAL ENGINEERING



## **Certificate**

Certified that the project entitled

**“Measurement of Laminar Flame Speed of LPG-Air Mixtures with  
Cylindrical Flame Tube Method”**

Carried out by:

Mr. ABHINANDAN D. KADAM

[USN: 2JI16ME002]

Mr. ANUP J. GOURGONDA

[USN: 2JI16ME703]

Mr. NIKHIL P. DAPHALE

[USN: 2JI16ME026]

Mr. SAJAN V. ASNOTIKAR

[USN: 2JI16ME012]

Bonafide students of **Jain College of Engineering, Belagavi**, in partial fulfillment for the award of **Bachelor of Engineering in Mechanical Engineering** from **Visvesvaraya Technological University, Belagavi**, during the academic year **2019-20**. It is certified that all corrections and suggestions indicated for internal assessment have been incorporated in the report. The project report has been approved as it satisfies the academic requirements in respect of project work prescribed for the said degree.

**Dr. M. Sreedhar Babu**

Guide

**Prof. D. B. Patil**

HOD

**Dr. K. G. Vishwanath**

Principal & Director

Examiner Sign:

1.

2.

# CONTENTS

	PAGE NO
ACKNOWLEDGEMENT	i
ABSTRACT	ii
LIST OF FIGURES	iii
LIST OF TABLES	iv
CHAPTER 1: INTRODUCTION	1
CHAPTER 2: LITERATURE REVIEW	
2.1 History of laminar burning velocity	3
2.2 Flame front propagation	5
2.3 Factors influencing the speed	6
2.3.1 Turbulence	
2.3.2 Fuel-Air ratio	
2.3.3 Effect of Compression Ratio	
2.3.4 Adiabatic Flame Temperature	
2.3.5 Effect of Initial Mixture Temperature	
CHAPTER 3: METHODS OF MEASURING FLAME SPEED	
3.1 Bunsen flame approach	14
3.1.1 Flame area method	
3.1.2 Flame angle method	
3.2 Spherically expanding flame method	16
3.3 stagnation flame approach	17
3.4 Flame tube method	18
3.5 Flames in tubes	20
3.6 Property table for LPG (Gaseous)	23

<b>OBJECTIVES:</b>	24
--------------------	----

## **CHAPTER 4: EXPERIMENTAL SETUP DESIGN FOR MEASURING FLAME VELOCITY**

4.1 Experimental setup	25
4.1.1 Flame tube	26
4.1.2 Flame arrestor	27
4.1.3 Calibrated Rotameters	27
4.1.4 Buffer tank	28
4.1.5 Ignition assembly	29
4.1.6 Pressure regulators	29
4.1.7 Domestic LPG cylinder	30
4.1.8 Zero air cylinder	31
4.1.9 Calibrated LPG cylinder	31
4.1.10 Mixing chamber	32
4.1.11 Pneumatic Tubing	32
4.1.12 Reducers and valves	33
4.1.13 Fire extinguisher	34
4.2 Modification of experimental setup	35

## **CHAPTER 5: MEASUREMENT OF FLAME VELOCITY**

5.1 Procedure to measure flame velocity	36
5.2 Comparing non calibrated rotameter readings with Calibrated rotameter readings	37
5.3 flame colors for different air fuel ratios	38

## **CHAPTER 6: PARTIAL AUTOMATION OF EXPERIMENTAL SETUP**

6.1 Arduino UNO	39
6.2 LDR (Light Dependent Resister) sensor	40

6.3 Wiring (Jumping cable)	40
6.4 LCD Display	41
6.5 Program developed to measure the flame velocity	42
6.6 Procedure after partial automation	43
 <b>CHAPTER 7: RESULTS AND DISCUSSION</b>	 44
 <b>CHAPTER 8: PROJECT EXPENDITURE</b>	 47
 <b>CHAPTER 9: GANTT CHART</b>	 48
 <b>CHAPTER 10: CONCLUSION</b>	 49
 <b>REFERENCES</b>	 50
 <b>APPENDIX</b>	 51

## ACKNOWLEDGEMENT

This has been the light of the day due to invaluable contribution of certain individuals whose constant guidance, support and encouragement resulted in the realization of our project.

We are grateful to our Guide **Dr. M. Sreedhar Babu** and HOD of Mechanical Engineering, **Prof. D. B. Patil** for providing us the necessary help and encouragement whenever we needed, which has resulted in success of our project.

We take this opportunity to thank **Dr. K. G. Vishwanath**, Principal of Jain college of Engineering, Belagavi for providing a healthy environment in the college, which helped us in concentrating on our task.

We would also like to thank all staff members of our department, without whose constructive suggestions and valuable advice, the simple idea, which had borne by us, would not have been able to blossom forth to give such a beautiful bloom.

Last but not the least, we are grateful to all our friends and our parents for their direct or indirect constant moral support throughout the course of this project.

**Batch: B8**

## **ABSTRACT**

One of the most attractive applications of Liquefied Petroleum Gas (LPG) is its use in domestic cooking and particularly for automotive applications, as it is known to be a clean source of energy. Even though it is already being used in IC engines, the fundamental combustion properties such as laminar burning velocities, which is a physiothermal property of a fuel, is still not very well established, which is required as fundamental basic input for engine modeling. The present work utilizes a few standard methods of flame speed measurement known from the literature to obtain the flame speed of LPG-air and LPG-air-diluents mixtures as a function of air-fuel ratio and diluents concentration. Other methods to determine the burning velocity such as Heat flux burner method, Flat flame burner method, Bunsen burner method, Slot burner technique, Counter flow diffusion flow, Soap bubble technique, and Tube propagating method.

## LIST OF FIGURES

<b>Fig No</b>	<b>Description</b>	<b>Page No</b>
2.1	Details of flame travel	6
2.2	The variation of burning velocity with equivalence ratio for several fuel-air mixtures at P=0.1MPa, T=298K	8
2.3	Graph of computational burning velocity vs. Experimental burning velocity	9
3.1	Burners flame with 3 standard optical accessible flame edges	15
3.2	Unburned flame speed based on half cone angle	15
3.3	Spherical flame front measurement	17
3.4	Schematic of the stagnation flow field with flame	18
3.5	Flame propagation apparatus	19
3.6	Flow pattern and particle velocity for a laminar combustion wave moving from open to closed end	20
3.7	Flow lines in a laminar combustion wave moving from open to closed end of a tube	21
3.8	Calculated shape of the flame and flow lines in a tube	21
3.9	Actual flame shapes in a horizontal tube open at the ignition end for propane-air mixtures	22
4.1	Experimental setup	25
4.2	Flame tube	26
4.3	Flame arrestor	27
4.4	Calibrated Rotameters	27
4.5	Buffer tank	28
4.6	Ignition assembly	29
4.7	Pressure regulator	29
4.8	Domestic LPG cylinder	30
4.9	Zero air cylinder	31



4.10	Calibrated LPG cylinder	31
4.11	Mixing Chamber	32
4.12	Pneumatic tubing	32
4.13	Reducers and Valves	33
4.14	Fire extinguisher	34
4.15	Fitting of calibrated rotameters	35
6.1	Arduino board	39
6.2	Detailed view of LDR sensor	40
6.3	Jumping Cable	40
6.4	LCD Display	41
6.5	Measurement chain system	43
7.1	Time V/s velocity plot	44
7.2	Propagation of flame front	45
7.3	Domestic LPG flame front	46
7.4	Calibrated LPG flame front	46

## LIST OF TABLES

<b>Table No</b>	<b>Description</b>	<b>Page no</b>
3.1	LPG Properties	23
4.1	List of components	26
5.1	Tabular column	37
5.2	Flame color analysis	38
7.1	Comparison of manual readings with sensor readings	44
7.2	Laminar flame speed for LPG-Air mixture	45
8.1	Project Expenditure	47
9.1	Gantt chart	48

## CHAPTER 1. INTRODUCTION

Liquefied petroleum gas or liquid petroleum gas (LPG or LP gas) which is used for domestic purpose and which is also widely used in IC engines yet its fundamental combustion properties such as laminar burning velocity is still not very well established, which can act as a basic input for engine modeling. One of the most important intrinsic properties of any combustible mixture is its laminar burning velocity. It depends on the mixture composition, temperature and pressure. systems. For instant, in the design of burners and combustion chamber of gas turbine, the flame speed must equal to the mixture flow velocity for a stable flame to be obtained. Three combustion velocities, that is, laminar burning velocity, spatial velocity of flame front and unburnt gas velocity are generally defined in any combustion system. Laminar burning velocity is defined as the velocity of the combustion wave normal to itself and relative to the unburnt gas. It is defined as volume of unburnt gas consumed per unit time divided by the area of the flame front in which that volume is consumed in a laminar premixed combustion process. In an engine, the burning velocity is usually higher than the corresponding laminar burning velocity due to presence of turbulence, which can be considered with the scale and intensity of turbulence. Lewis and Elbe suggested that the laminar burning velocity, ignition delay and engine knock are correlated. A fairly large number of researchers have been engaged in this field for the last decades. Fells and Rutherford used Schlieren method to determine the laminar burning velocity of methane-air mixture, with and without diluents. He used both sharp edged orifice and bell shaped nozzle and compared the result of two types of burners. Gorden and Heimel determined the flame speed of methane-air, propane-air, and ethylene-air mixtures at low initial temperatures. They used shadowgraph method for nozzle type burner. Fine determined stability limit and burning velocities of hydrogen air flames at reduced pressure. From the above survey, it was found that various kinds of burners have been tried like circular tube, shaped nozzle, orifice and rectangular slot type. It was found that in circular tube and rectangular slot type, the unburnt gas velocity profile is parabolic, while orifice burners yield essentially uniform velocity profiles and straight-sided flame cones. Kanitkar determined experimentally the flame speed, temperature and limits of flame propagation for producer gas-air mixture. They used flame tube method with its one end opened for exhaust gas removal and other end closed after filling the tube with required air fuel mixture. The method used by Coward and Hartwell consists of law of

cylindrical tube closed at one end and filled with the gas mixture under test. The present paper analyses the laminar burning velocity of LPG-air and LPG-air and diluent mixture using the burner method. Flame arrestor, orifice burner and its assembly were designed for analyzing the laminar burning velocity. Various results for laminar burning velocity of LPG-air and LPG, air and  $CO_2$  mixtures were obtained at atmospheric pressure using burner method and results were compared with the standard available data for methane, ethane and propane.

## CHAPTER 2. LITERATURE REVIEW

### 2.1 HISTORY OF LAMINAR BURNING VELOCITY

The velocity of combustion wave normal to itself and relative to unburnt gas is said to be laminar burning velocity. It is also defined as volume of unburnt gas consumed per unit time divided by the area of the flame front in which that volume is consumed in a laminar premixed combustion process. Researchers have developed many techniques to measure the laminar burning velocity of various fuel + air mixtures. In spherical flame method, the fuel air mixture ignites the centre using a spark and flame propagation speed is determined either from pressure-time history or flame radius with time. In stagnation flame method, the minimum flow velocity near the stabilized flame is considered as flame propagation velocity. The measured flame propagation speeds from these methods are corrected to flame stretch to derive laminar burning velocity. Heat-flux method helps direct measurement of laminar burning velocity by stabilizing an adiabatic planar flame on the top of a perforated plate. Burner method annular stepwise diverging tube and diverging channel method uses mass conservation across the flame front to derive laminar burning velocity of premixed fuel + air mixtures.

Premixed flames were used in chemical laboratories as early as in 18<sup>th</sup> century; however, only in 1854 Bunsen proposed a design suitable for stabilization of the flames of different composition and their investigation. First measurements of the flame burning velocity of hydrogen and carbon monoxide were performed by Bunsen in 1867 using eudiometer fitted with electrodes to ignite a mixture of gas. Subsequently; Mallard measured burning velocity of fire-dump and lightning gases using the same method and proposed the first flame propagation theory in 1875, which was later developed by Mallard and Le Chatelier.

Mason and Wheeler also investigated flames propagating in tubes and discovered that flame propagation speed depends on the tube diameter. Further attempts to improve this method, notably by Coward and Hartwell demonstrated that flames propagating in tubes are not flat and attempted to take the flame front surface in to consideration to derive average burning velocity.

Gouy implemented Bunsen burner and suggested that in conical flames, the burning velocity can

be defined as volumetric rate of flow divided by the area of the flame surface. When the flame shape is close to conical, this yields sine angle based method. The same approach was later discussed by Michelson, who contributed to the development of the theory of Mallard and Le Chatelier. Hopkinson reported first experimental investigation of flame propagation in a confined chamber with central ignition by electric spark. Flamm and Mache were first to propose a relation between pressure and the amount of mixture burnt for spherical flames.

Soap bubble method based on spherical flames was proposed by Stevens and further developed by Fiock and Marvin. Ellis and Wheeler reported the first photograph of spherical flames simultaneously with pressure measurements. Lewis and von Elbe proposed measurement of laminar burning velocity,  $S_L$  with constant volume spherical flame method from time pressure explosion records.

In 1943, Lewis and von Elbe, introduced particle imaging based technique to understand the laminar burning velocity behavior within the burner stabilized flames. Laminar burning velocity measurement using planar flame front was proposed by Powling.

In particular, the laminar flame speed,  $S_{Lo}$ , represents the rate at which the fresh gases are consumed through the flame front considering a 1D unstretched propagating planar premixed flame. It is a fundamental flame property which depends only on the fuel/air mixture and its initial thermodynamic conditions: pressure, temperature and equivalence ratio. Flame speed is a global indicator for the reactivity of a specific mixture of fuel and air. This parameter has been extensively studied for more 70 years and at the beginning of the flame speed experimentations, the measurements were mostly concentrated to simple gaseous mixtures like for example, methane/air, hydrogen/air or small molecular weight fuels at standard conditions of temperature and pressure. During this early period of combustion research, flame speed measurements were less accurate and very scattered (up to 20 cm/s between results). Data scattering began to significantly reduce from 1980s when the aerodynamic stretch effects were well quantified. Now a day the discrepancy between flame speed measurements are expected to be around 5 cm/s and it has to be still more reduced in a next future.

In the last several years, the interest in measuring the laminar flame speed continues to increase due to the relevance of  $S_{Lo}$  to kinetic model development and to high-pressure combustion.

Many experimental approaches have been developed within this context: the steady burner-stabilized flames, the steady stagnation-type flames and the unsteady spherically expanding flames.

## 2.2 FLAME FRONT PROPAGATION

For efficient combustion the rate of propagation of the flame front within the cylinder is quite critical. The two important factors which determine the rate of movement of the flame front across the combustion chamber are the reaction rate and the transposition rate. The reaction rate is the result of a purely chemical combination process in which the flame eats its way into the unburned charge. The transposition rate is due to the physical movement of the flame front relative to the cylinder wall and is also the result of the pressure differential between the burning gases and the unburnt gases in the combustion chamber.

Figure 2.2 shows the rate of flame propagation. In area 1, (A→B), the flame front progresses relatively slowly due to a low transposition rate and low turbulence. The transposition of the flame front is very little since there is a comparatively small mass of charge burned at the start. The low reaction rate plays a dominant role resulting in a slow advance of the flame. Also, since the spark plug is to be necessarily located in a quiescent layer of gas that is close to the cylinder wall, the lack of turbulence reduces the reaction rate and hence the flame speed. As the flame front leaves the quiescent zone and proceeds into more turbulence areas (area2) where it consumes a greater mass of mixture, it progresses more rapidly and at a constant rate (B→C) as shown in Figure. The volume of unburned charge is very much less towards the end of flame travel and so the transposition rate again becomes negligible thereby reducing the flame speed. The reaction rate is also reduced again since the flame is entering a zone area (area 3) of relatively low turbulence (C→D) in Figure.

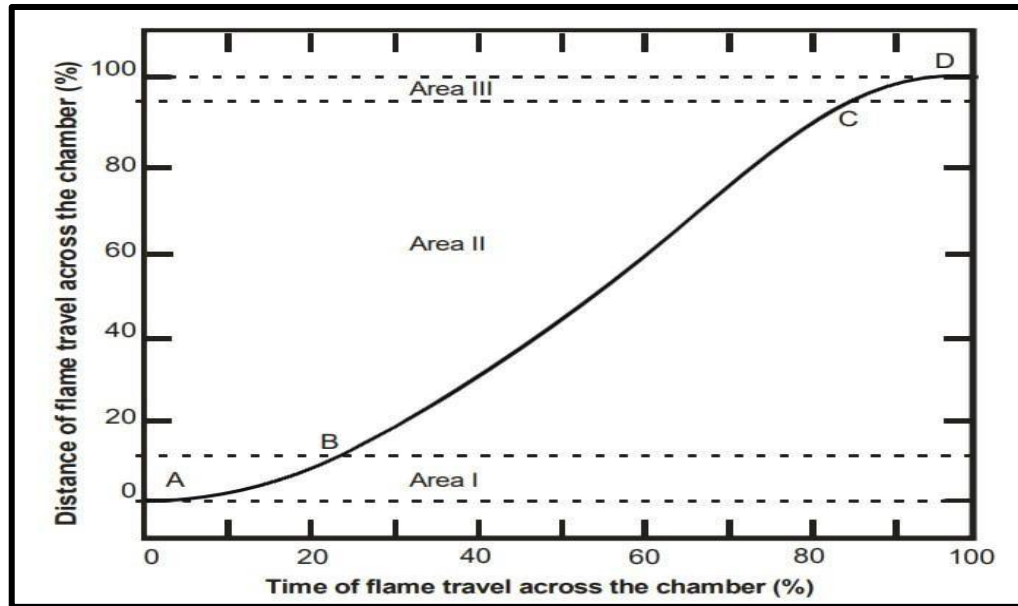


Fig. 2.1 Details of flame travel

## 2.3 FACTORS INFLUENCING THE FLAME SPEED

The study of factors which affect the velocity of flame propagation is important since the flame velocity influences the rate of pressure rise in the cylinder and it is related to certain types of abnormal combustion that occur in spark-ignition engines. There are several factors which affect the flame speed, to a varying degree, the most important being the turbulence and the fuel-air ratio. Details of various factors that affect the flame speed are discussed below.

### 2.3.1 TURBULENCE

The flame speed is quite low in non-turbulent mixtures and increases with increasing turbulence. This is mainly due to the additional physical intermingling of the burning and unburned particles at the flame front which expedites reaction by increasing the rate of contact. The turbulence in the incoming mixture is generated during the admission of fuel- air mixture through comparatively narrow sections of the intake pipe, valve openings etc., in the suction stroke. Turbulence which is supposed to consist of many minute swirls appears to increase the rate of reaction and produce a higher flame speed than that made up of larger and fewer swirls. A suitable design of the combustion chamber which involves the geometry of cylinder head and piston crown increases the turbulence during the compression stroke.



### 2.3.2 FUEL-AIR RATIO

The fuel air ratio has a very significant influence on the flame speed. The highest flame velocities are obtained with somewhat richer mixture. When the mixture is made leaner or richer the flame speed decreases. Less thermal energy is released in the case of lean mixtures resulting in lower flame temperature. Very rich mixtures lead to incomplete combustion which results again in the release of less thermal energy. The experimental burning velocity data for several fuel-air systems is plotted in Fig. against equivalence ratio (fuel/air mixture). It can be noted that for typical hydrocarbon-air systems, the burning velocity varies in the range of 25-50 cm/s. The peak burning velocity occurs near stoichiometric or slightly fuel rich mixture ( $\phi = 1.05$ ) in most hydrocarbon-air flames and drops down both on the lean and rich sides. However, the maximum burning velocity for hydrogen-air mixture occurs under fuel rich mixture around  $\phi=1.8$ . For rich mixture ratio, some left over hydrogen is likely to be present in the mixture.

The molecular weight of hydrogen is low and burning velocity is inversely proportional to molecular weight ( $S_L \propto MW^{-1}$ ), the maximum burning velocity is likely to occur under fuel-air conditions. It is interesting to note from Fig. that CO air mixture also attains maximum value of burning velocity under fuel rich mixture ratio (around  $\phi=2.0$ ) like that of the  $H_2$ -air flame. This CO air burning velocity data is unique and is not yet understood due to its complex chemical kinetics. Though the peak adiabatic flame temperature is roughly the same particularly for hydrogen-acetylene and CO air mixtures. But the peak burning velocities of these fuel-air mixtures are quite different and this cannot be explained in terms of molecular weight. These glaring differences are attributed to different chemical kinetics for these fuel-air mixtures. Both the overall pre-exponential factor and effective value of activation energy are quite different for these mixtures.

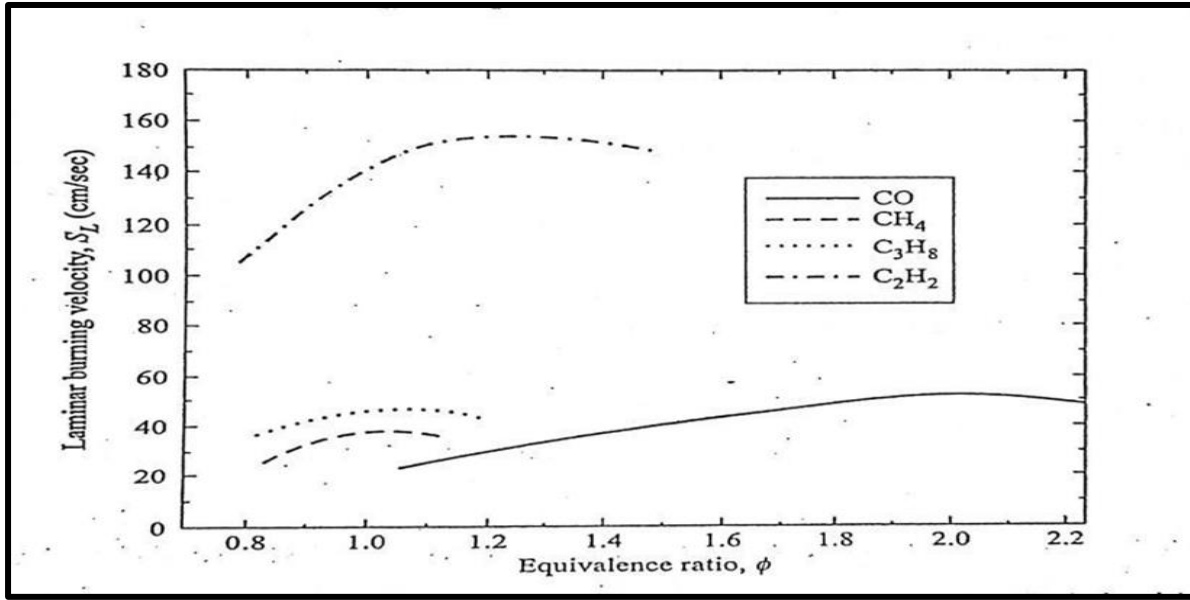


Fig. 2.2 The variation of burning velocity with equivalence ratio for several fuel-air mixtures at  $P = 0.1$  MPa,  $T = 298$  K

### 2.3.3 EFFECT OF COMPRESSION RATIO

A higher compression ratio increases the pressure and temperature of the working mixture which reduce the initial preparation phase of combustion and hence less ignition advance is needed. High pressures and temperatures of the compressed mixture also speed up the second phase of combustion. Increase compression ratio reduces the clearance volume and therefore increases the density of the cylinder gases during burning. This increases the peak pressure and temperature and total combustion duration is reduced. Thus engines having higher compression ratios have higher flame speeds.

According to S.Y. Liao et al carried out the study on Determination of the laminar burning velocities for mixtures of ethanol and air at elevated temperatures. It has measured the laminar burning velocities for ethanol-air premixed flames at various temperature and equivalence ratio. The flames are analyzed to estimate flame size, consequently, the flame speeds are derived from the variations of the flame size against the time elapsed. It was studied the effects of the fuel/air equivalence ratio, initial temperature and pressure on the laminar flame propagation. It was conducted the premixed laminar combustion of ethanol-air mixture experimentally in a closed combustion bomb. And it was found the laminar burning velocity 58.3 cm/s at normal pressure of 0.1 MPa and temperature of 358K. Xuan Zhang et al carried out the study on Measurements of

laminar burning velocities and flame stability analysis for dissociated methanol–air–diluent mixtures at elevated temperatures and pressures. In this the laminar burning velocities and Markstein lengths for the dissociated methanol–air–diluent mixtures were measured at different equivalence ratios, initial temperatures and pressures. The influences of these parameters on the laminar burning velocity and Markstein length were analyzed. It was found that the peak laminar burning velocity occurs at equivalence ratio of 1.8. The Markstein length decreases with an increase in initial temperature and initial pressure. Measurements of laminar burning velocities and flame Stability analyses are conducted using the outwardly spherical laminar premixed flame for DM–air and DM–air–diluent mixtures. The laminar burning velocity and Markstein length at different equivalence ratios, initial temperatures, initial Pressures and  $N_2/CO_2$  dilution ratios are obtained. Erjiang Hu et al carried out the numerical study on laminar burning velocity and NO formation of the premixed methane–hydrogen–air flames.

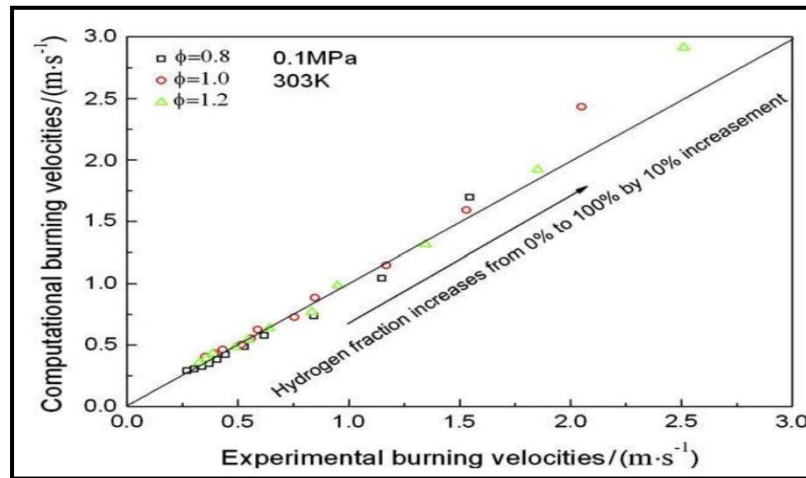


Fig 2.3 Graph of computational burning velocity vs Experimental burning velocity

It was found that the unstretched laminar burning velocity is increased with the increase of equivalence ratio and it decreases as the mixtures become fuel-rich.

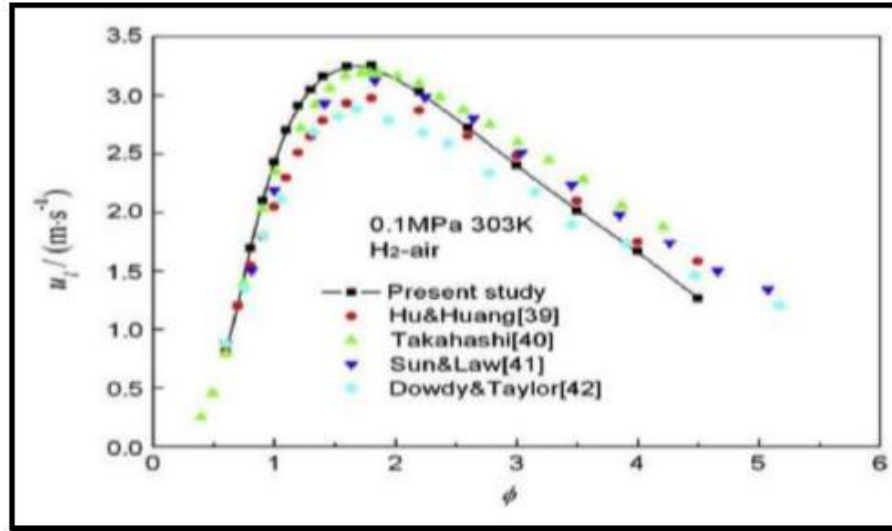


Fig 2.4

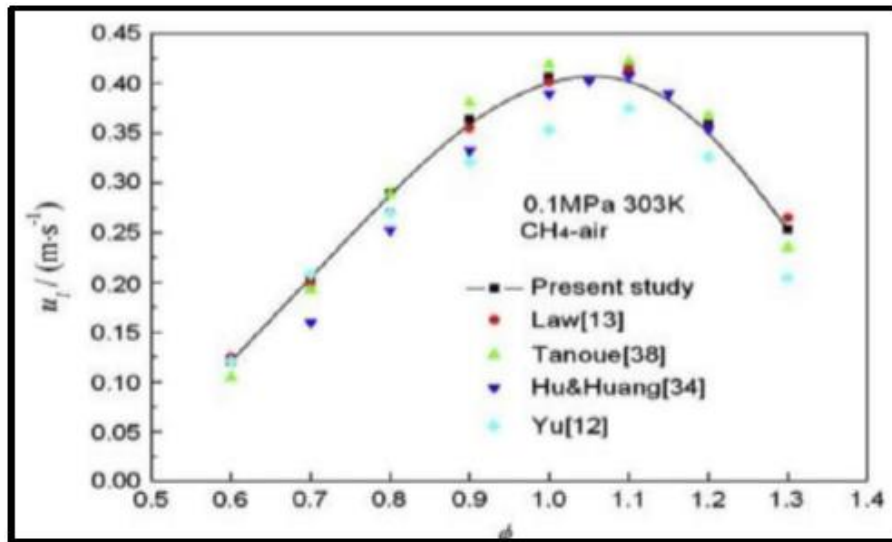


Fig 2.5

Peak value of unstretched laminar burning velocity of methane–air mixture is presented at the equivalence ratio of 1.1 and that of hydrogen–air mixture is presented at equivalence ratio of 1.8. Methane dominated combustion is presented when hydrogen fraction is less than 40%, where laminar burning velocity is slightly increased with the increase of hydrogen addition. When hydrogen fraction is larger than 40%, laminar burning velocity is exponentially increased with the increase of hydrogen fraction. With the increase of hydrogen fraction, the overall activation energy of methane–hydrogen mixture is decreased, and the inner layer

temperature and Zeldovich number are also decreased. All these factors contribute to the enhancement of combustion as hydrogen is added.

### 2.3.4 ADIABATIC FLAME TEMPERATURE

The first parameter of interest is adiabatic flame temperature ( $T_{ab}$ ). It is defined as the equilibrium temperature of the products when the reactants are burned at constant pressure without any heat transfer to the surroundings. In flames, the reactants are converted to products essentially at constant pressure, thus the maximum temperature of the flame is typically close to the adiabatic flame temperature (in the absence of non-unity Lewis number, differential diffusion and strain effects). Flame temperature is an important parameter for a number of reasons; for example,  $NO_x$  production is highly sensitive to temperature through the thermal (Zeldovich) mechanism, which tends to dominate  $NO_x$  production beyond 1800 K. More to the point for the current study, the flame temperature can also have a significant influence on flame speed. Figure 2.1 compares the adiabatic flame temperatures for different pure fuel gases ( $CH_4$ ,  $H_2$  and  $CO$ ) with a typical syngas fuel mixture. The chosen syngas fuel composition is 35%  $H_2$ , 35%  $CO$  and 30%  $CO_2$ , as many syngas fuel sources produce mixtures with comparable amounts of  $H_2$  and  $CO$ , and with significant levels of added diluents ( $CO_2$ ,  $H_2O$  and  $N_2$ )

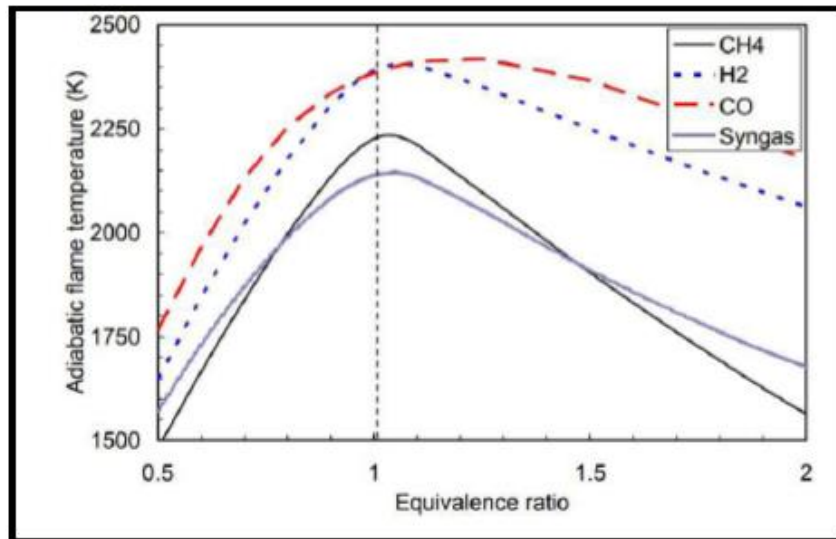


Fig 2.6 Adiabatic flame temperature for  $CH_4$ ,  $H_2$ ,  $CO$  and typical Syngas (35 %  $H_2$ , 35%  $CO$ , 30%  $CO_2$  fuels with air.)

For all the fuels, the adiabatic flame temperature peaks around stoichiometric conditions. The highest flame temperature for a given equivalence ratio, while CH<sub>4</sub> has the lowest. At  $\Phi=0.6$ , the CO flame temperature is around 300 K higher than for CH<sub>4</sub>, and the differences are even greater on the rich side.

Methane-air mixtures have lower flame temperatures than CO and H<sub>2</sub>, because CH<sub>4</sub> requires four times more oxidizer (on a molar basis) to achieve a stoichiometric mixture. For an undiluted oxidizer (e.g., pure O<sub>2</sub>), the CH<sub>4</sub> flame temperatures are much closer to the other fuels. Though both CO and H<sub>2</sub> require the same amount of oxidizer for a given equivalence ratio, the CO flame temperature is slightly higher than for H<sub>2</sub>, owing to the higher heating value of CO (on a molar basis). At  $\Phi=0.6$ , the CO flame temperature is around 130 K more than hydrogen's. This difference is greatly reduced as the mixture nears stoichiometric conditions, since the higher temperatures there lead to reduced 2 levels, and therefore less heat release associated with the additional fuel.

The syngas flame temperature is lower than that for either H<sub>2</sub>, or CO due to the significant amount of diluents in the syngas. For the 30% CO<sub>2</sub> dilution considered here, the flame temperature is similar to that for the CH<sub>4</sub> flame (less than ~100 K difference) over the range of practical equivalence ratios. Thus, we see that undiluted syngas mixtures would have higher temperatures than conventional methane (or natural gas) fuel, while syngas compositions with typical levels of dilution will have flame temperatures closer to those encountered in methane combustion.

### **2.3.5 EFFECT OF INITIAL MIXTURE TEMPERATURE**

The effect of initial mixture temperature on burning velocity has been investigated extensively. The experimental data obtained by Mishra is shown fig. against initial mixture temperature for three hydrocarbon-air mixtures.

From these results, burning velocity and the initial temperature of the mixture can be related as  $SL \propto T_{in}^m$  with the exponent,  $m$  ranging from 1.5-2. The increase of SL with  $T_{in}$  is caused by

preheating of the mixture. But the preheating of the mixture would not enhance the flame temperature significantly. However, a slight change in TF alters SL significantly as it appears in the exponential term of the reaction rate expression.

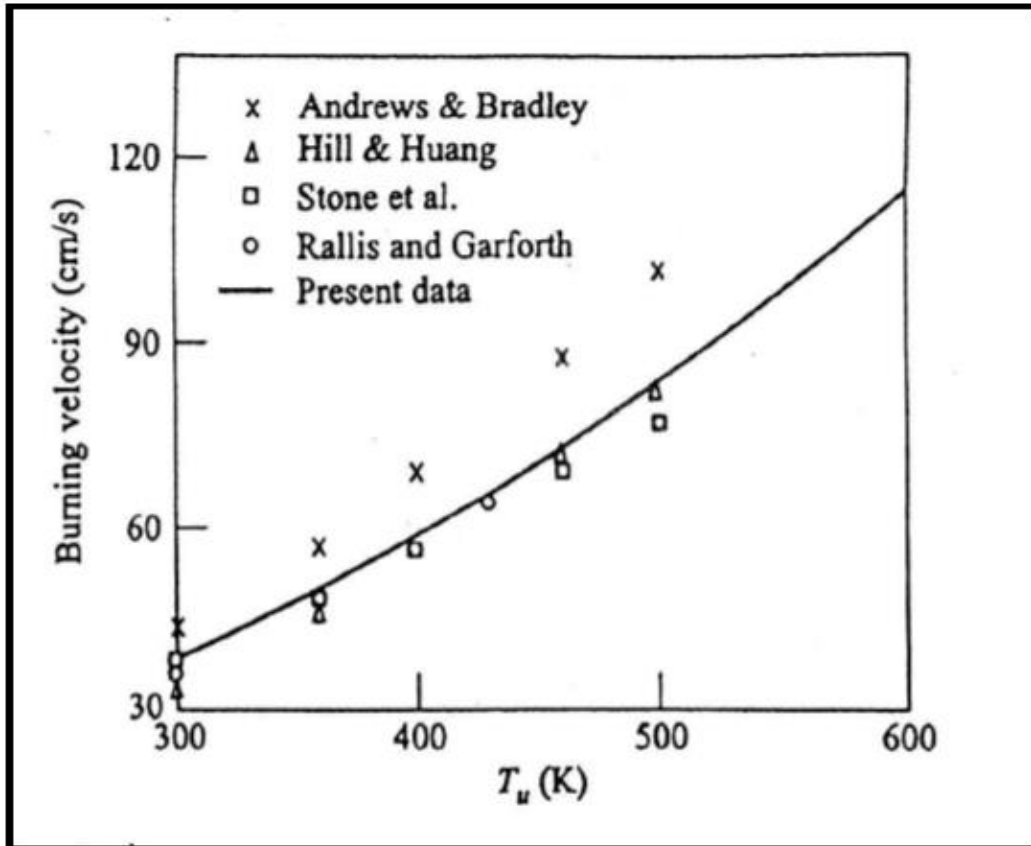


Fig. 2.7. Effect of initial mixture temperature

## CHAPTER 3. METHODS OF MEASURING FLAME SPEED

1. Bunsen burner method
2. Spherical flame method
3. Stagnation flame method
4. Flame tube method
5. Diverging channel method
6. Soap bubble method

### 3.1 BUNSEN'S FLAME APPROACH

This approach typically uses a 2-d or axis-symmetric conical premixed flame, stabilized on the lip of a slot burner or a straight cylindrical tube, respectively. This conical flame is affected by hydrodynamic strain (tangential velocity gradient along the flame surface) and pure curvature (at reactant mixture. The main disadvantage of the flame tip and azimuthal curvature for 3D conical flame), and their combined influence on local flame speed depends on the Markstein length of this approach is that it neglects the influence of the stretch on the measured flame speed. There are two popular methods to deduce the flame speed from these conical flames:

- (1) Flame area method
- (2) Flame angle method.

#### 3.1.1 Flame area method by Bunsen's method

The average flame speed ( $S$ ) calculated in this method is an area weighted flame speed over the entire flame surface. Considering the overall mass balance, the average flame speed is calculated by dividing the volume flow rate of the mixture with the surface area of the flame.

$$\dot{m} = \rho S A \text{ or } S = \frac{\dot{Q}}{A}$$

While the rim stabilized conical flame is not truly adiabatic, because of heat losses to the burner rim (as well as some radiation losses), the effect should be small as the heat loss is confined primarily to the base of the flame. Also, the effect of rim heat loss should be independent of



burner size as the flame volume from which heat is lost is proportional to the rim area where  $m$  and  $Q$  are the measured mass and volume flow rates of reactants through the burner, and  $\rho$  and  $A$  are the unburned density and conical flame surface area at appropriately chosen.

The choice of location is a concern as it gives a wide range of flame surface area and hence measured flame speed. Traditionally, there are three flame edges used for flame area calculation: (1) schlieren (first derivative of density), (2) inner edge of shadowgraph (second derivative of density), and (3) visible (chemiluminescence) edge. From the definition of the unburned laminar flame speed, the apparent flame area should be the unburned flame area, which is just upstream of the preheat zone of the flame. Hence, the inner edge of shadowgraph images or schlieren edges have been preferred over the visible (chemiluminescence) for flame area calculation as they are closer to the unburned boundary.

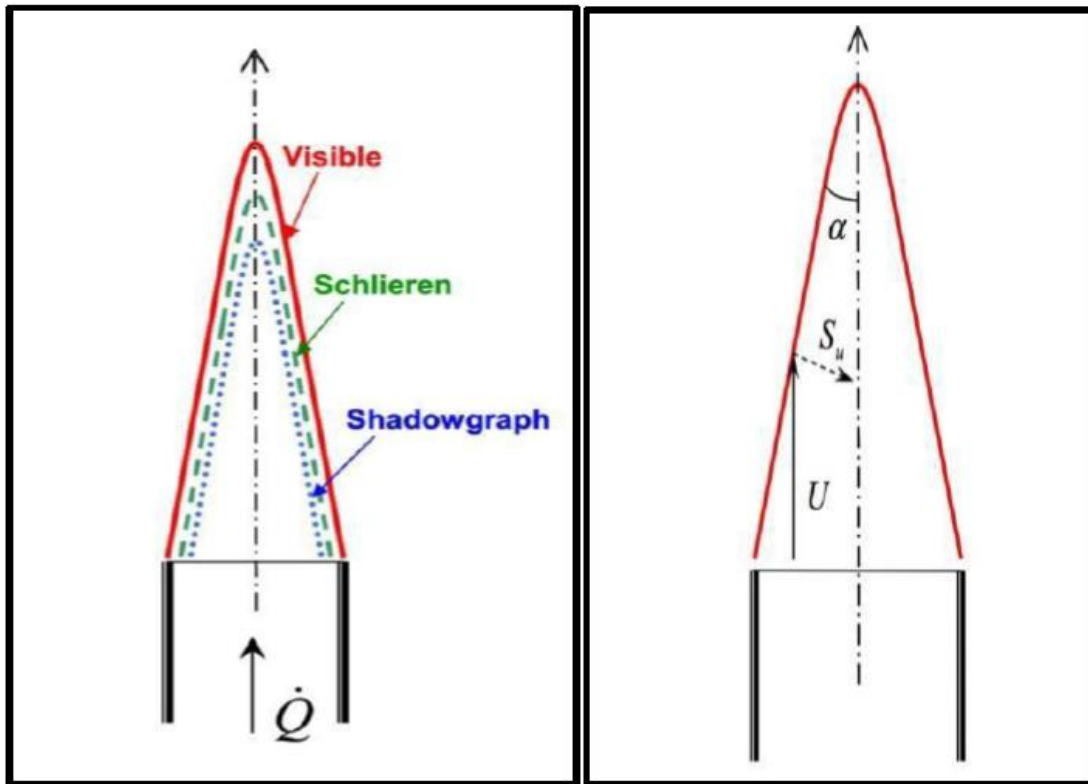


Fig. 3.1 Burners flame with 3 standard optical accessible flame edges

Fig. 3.2 Unburned flame speed based on half cone angle

Specifically, the inner edge of the shadowgraph image of the flame has been assumed to give the best result of all three as it is the closest to the unburned surface of the flame. It should be noted that the flame cone can act as a lens in the shadowgraph, which raises the uncertainty in the measured flame area. It is important to point out; however, that the use of the unburnt flame area does not result in a measurement of the 1-d unstretched unburnt flame speed, as the unburned surface is strongly affected by curvature and strain.

### 3.1.2 Flame angle method

In this method, the angle subtended by the flame edge to the unburned incoming flow velocity in the shoulder region of the conical flame is measured and the flame speed is calculated by,

$S_u = U \sin \alpha$  where  $U$  is the unburned gas velocity and  $\alpha$  is the half cone angle as shown in above Fig.. A conical flame stabilized on a contoured nozzle is preferred over straight cylindrical tube burner for the following reason. The exit velocity profile of a long cylindrical tube is parabolic and hence the flame angle ( $\alpha$ ) to the incoming flow varies along the flame height. Whereas, a contoured nozzle produces a nearly uniform exit velocity profile, which gives a fairly straight edge along the shoulder of the flame to determine the half cone angle more accurately. The main drawback of this method, apart from the measurements not corrected for stretch, that there is a huge uncertainty even if there is a small divergence in the streamline approaching the flame.

## 3.2 SPHERICALLY EXPANDING FLAME METHOD

A freely expanding spherical flame in a nominally constant pressure vessel is used for stretch corrected flame speed measurement as shown in Figure 3.2. This spherical flame is a positively stretched flame as the flame area increases with time. The stretch ( $K$ ) imposed on the flame is due to the flame motion and can be calculated from

$$\frac{2}{R_f} \frac{dR_f}{dt} \text{ ----- (i)}$$

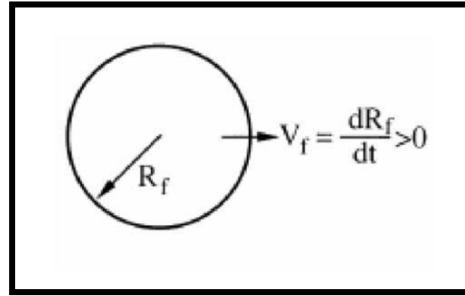


Fig. 3.3 Spherical flame front measurement

$$k = (\mathbf{v}_f \cdot \mathbf{n})(\bar{\mathbf{v}} \cdot \mathbf{n}) = v_f = \frac{dR_f}{dt} \text{ ----- (ii)}$$

Where  $v_f$  is the flame front velocity,  $R_f$  is the radius of the flame front at time  $t$ . The products inside the spherical flame are at rest in the laboratory frame of reference. Since the products are not moving (on average), the velocity of the flame propagation ( $v_f$ ) is nothing but the burned flame speed ( $S_b$ ). From continuity and assuming that the flame is quasi-steady, the unburned flame speed ( $S_u$ ) is calculated from  $S_u = S_b \left( \frac{\rho_b}{\rho_u} \right)$

### 3.3 STAGNATION FLAME APPROACH

A steady 1-D strained laminar flame stabilized in a well-defined stagnation flow field is used for measurements in this approach. The stagnation flow field is achieved either by impinging two identical nozzle-generated flows or by impinging a generated flow with a solid wall. The stretch imposed on the flame is due to the non-uniformity (divergence) of the upstream flow or the hydrodynamic strain, which is represented by  $K = \bar{\mathbf{v}}_t \cdot \mathbf{v}_{s,t}$ . The flame speed and the imposed strain rate on the flame are determined from the axial velocity profiles across the flame.

Typically, the axial velocity decreases from the nozzle exit due to the presence of the stagnation plane, and it reaches a minimum before the flame. As the flow enters the flame, due to preheating and thereby thermal expansion, the axial velocity increases and reaches a maximum just after the peak of the heat release. After the heat release, the axial velocity decreases to zero at the stagnation plane. Commonly, the minimum velocity before the preheat zone is considered as the reference strained unburned flame speed ( $S_u$ ), and the maximum gradient of the axial velocity ahead of the minimum velocity location is taken as the imposed strain rate ( $K$ ).

The influence of strain on the flame speed  $S_u$  is subtracted by evaluating the flame speeds at various strain rates and taking advantage of the (typically) linear relationship between the flame speed and the imposed strain rate,

i.e.  $S_u = S_{u_0} - L_M \kappa$  especially at lower strain rates. The strained flame speed linearly extrapolated to zero strain rate is used to represent the unstrained flame speed ( $S_u$ ), while the slope of the linear fit ( $L_M$ ) represent the Mark stein length or strain sensitivity of the mixture. Like the spherically expanding flame method, this method measures the stretch corrected unburned flame speed and also the strain sensitivity of the fuel mixtures.

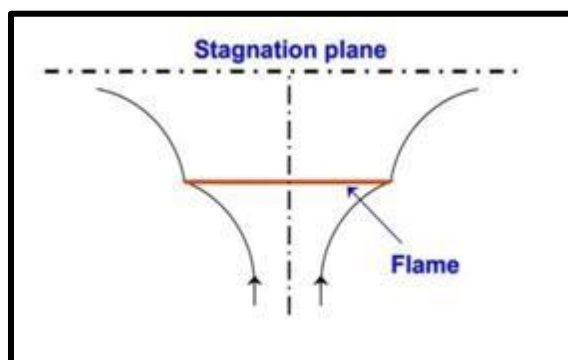


Fig. 3.4 Schematic of the stagnation flow field with flame

### 3.4 FLAME TUBE METHOD

This is one of the simplest and oldest method used first by Mallard and Le Chatelier, way back in 1883. In this method the combustible mixture is filled in a tube as shown in Figure. The inner diameter of the tube must be greater than critical diameter below which the flame is quenched. If the mixture is ignited at one end of the tube, by using a spark, a flame is initiated which propagates through the tube (see Fig. 3.4). Note that the flame will be the planar in the early stage and becomes curved as it moves further downstream towards unburnt mixture due to buoyancy effect.

It can be readily observed from Figure that the flame attains a parabolic flame shape, which results due to the following two factors:

- (i) Natural convection distorts the planar flame front, due to the difference in densities of burned and unburnt mixtures.

(ii) Due to friction at tube wall, the flame front travels at a higher velocity along the tube axis, which causes the flame front to be parabolic in shape. A suitable opening must be made at one of the tube to reduce reflected pressure waves which in turn would ensure uniform linear flame front velocity measurement over a large portion of the tube. This also helps in maintaining a constant shape of the flame front. The burning velocity  $s_L$  can be estimated as

$$s_L = v_F - \left( \frac{A_t}{A_f} \right) \text{ OR } s_L = (\rho_b / \rho_u)(dx / dt) \text{ ----- (iii)}$$

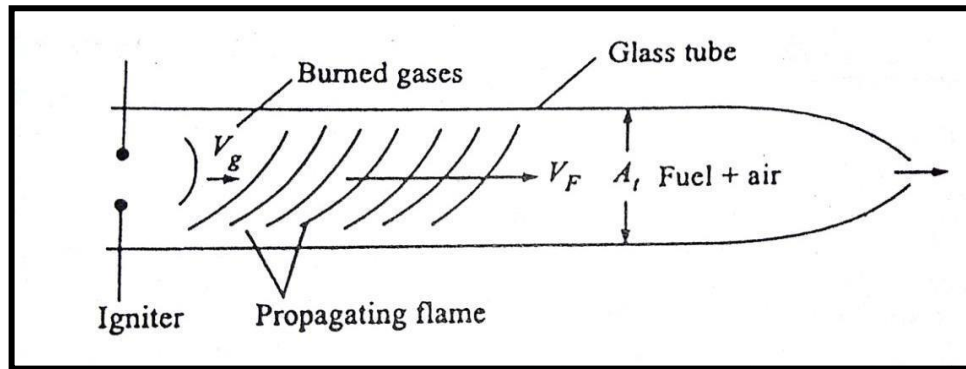


Fig. 3.5 Flame propagation apparatus

where  $V_F$  is the flame front velocity,  $V_g$  is the velocity of unburnt gas ahead of the flame,  $A_t$  is the cross-sectional area of the tube and  $A_f$  is the flame surface area. The magnitude of  $V_g$  can be estimated easily from the movement of the soap bubble front at the end of the tube. It must be noted that this is not very accurate method due to wall effects and distortion of flame surface as a result of buoyancy effect. Of course the buoyancy effect can be reduced considerably by using a vertical tube, particularly when the flame is allowed to move from top to bottom. If the flame travels from bottom to top vertically; the flame will be accelerated due to gas expansion and buoyancy effect.

### 3.5 FLAMES IN TUBES

The flame propagation rate was first measured by the time taken by a flame propagating between two fixed points in a tube. Gouy's definition of burning velocity brought the concept of flame shape and size. Coward and Hartwell's studied the shape of a flame in a tube and suggested that if each element of a flame consumes some amount of the combustible mixture, initial curve shift flame will ultimately assume a flat shape. So this suggested that the convection currents cause a small movement of gases ahead of the flame which resists the tendency of the flame to assume a flat shape.

If, in a tube with one end closed and filled with a combustible mixture, the mixture is ignited at the open end, a flame will travel towards the closed end. As a result of conversion, the burnt gases expand and move towards the open end and as there is no other opening. The burnt gases flowing in a tube have a Poiseuille type flow with maximum velocity at the centre and the low velocity near the walls on account of frictional drag. The accelerated rate flow near the axis of tube results in a central thrust towards the closed-end. This pushes the unburned gases from the central portion towards the walls. This results in the flow pattern shown in below figure.

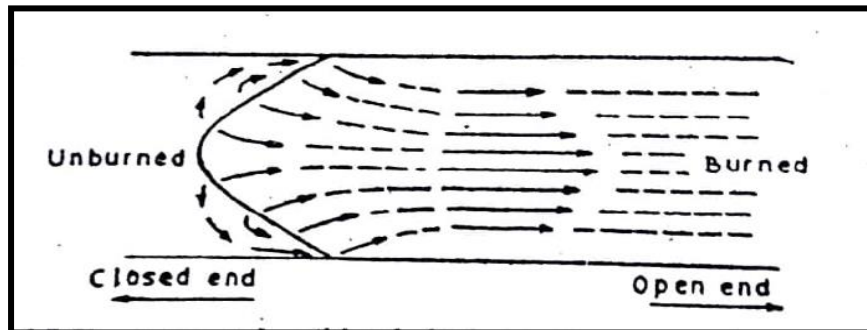


Fig.3.6 Flow pattern and particle velocity for a laminar combustion wave moving from open to closed end.

This gives the direction of the gas flow of the combustion wave and the magnitude and direction of the burnt gases flowing towards the open end.

If a stationary flame is maintained in a tube by allowing the mixture to flow with constant velocity, the flow pattern as shown in the figure will be obtained. Similar results of the gas flow pattern in a tube are obtained by the use of the particle track method. However, the flame shape is slightly different because the wall quenching effect reduces the burning velocity near the walls of the tube.

Frank Kamenetsky discuss the flame shape in a tube and suggested that if the walls of the tube are hot and the heat is flowing from outside to inside, the curvature of flame will be towards the burned side. but if the heat is flowing out from the conversion wave to the walls of the tube, the curvature of flame will be towards the unburned gas.

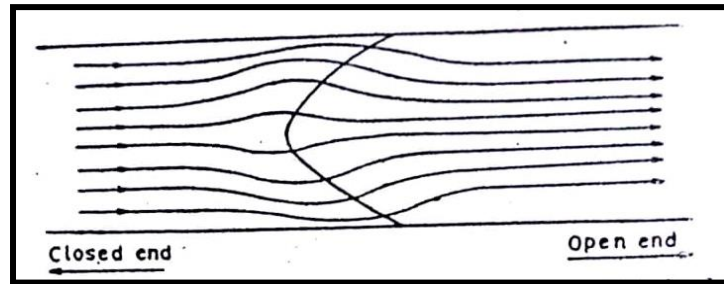


Fig.3.7 Flow lines in a laminar combustion wave moving from open to closed end of a tube.

Ball" calculated the shape of the flame on hydrodynamic considerations alone and gives the shape of flame and gas flow pattern as shown in the Fig.3.8. In the calculation assume the flame to be of zero thickness, constant burning velocity across the entire cross section, gases as ideal gases, and flow to be incompressible. As the solution was not exact his calculations did not give a precise description of the flame shaped at the tip and the near the wall.

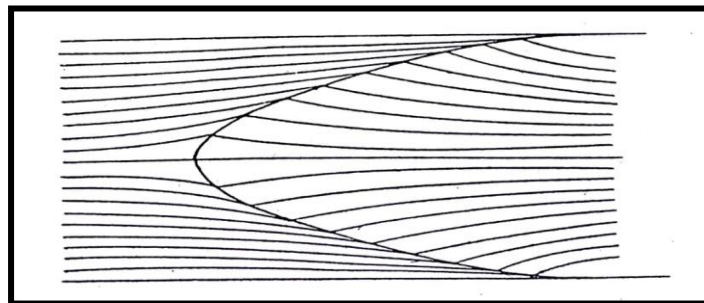


Fig.3.8 Calculated shape of the flame and flow lines in a tube

The first order analytical solution indicated the flame to be perpendicular to the axis at the tip and tangent to the walls. However, because of the quenching effect of the wall, Ball's assumption of constant burning velocity near the wall is not valid. The shape of flame and flow pattern obtained by him resembles the one obtained experimentally as shown in Fig.3.7.

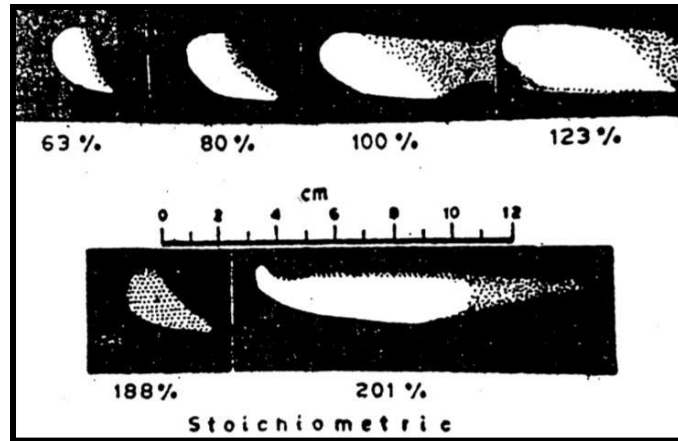


Fig.3.9 Actual flame shapes in a horizontal tube open at the ignition end for propane-air mixtures. The actual flame, in a horizontal tube with one end closed and where the mixture ignited by a spark at the open end, is hook shaped as shown in Fig.3.9.

It is observed that the shape of the flame is independent of the mode of ignition. If the spark is located at the bottom of the tube, an inverted hook shape is developed, but within a few centimeters of flame travels the shape changes to the normal hook shape. If the mixture is ignited by a pilot flame, hot body, or Spark located at any other position, the shape of the flame is same after it has propagated a distance of a few centimeters. The flame is hook shaped and unsymmetrical because of the convection current of hot gases. It is also observed that for most of the hydrocarbon-air mixture, near the maximum burning velocity, the flame shaped is constant in a 2.54 CM diameter tube. It is further reported that by placing an orifice at the open end of the tube the fluctuations in the flame shape reduced as it absorbs the pressure disturbance. By placing a second orifice at the closed end and thus permitting of flow of compressed unburned gas to the atmosphere also stabilizes the flame shaped. If the tube is very long or the diameter large, then after some travel the flame becomes turbulent. The turbulence can be avoided by using a tube of smaller diameter or tube of short length thus reducing Reynolds flow number.

The flame shaped is observed to change near the Lean and rich side of the mixture. If the mixture is quite rich the flame assumes an elongated shape which does not touch the bottom of the tube. Several other flame shapes are also obtained, the explanation of which is difficult. It is observed that the oscillation of the gas column in a hole can produce oscillations in the flame travel which do not change the shape of the flame.



### 3.6 PROPERTY TABLE FOR LPG (GASEOUS)

Table 3.1 LPG properties

Sl. No.	Parameters	Values
1.	Boiling point	-42°C
2.	Freezing point	-188°C
3.	Specific gravity	0.495 kg/m <sup>3</sup> at 25°C
4.	Adiabatic flame temperature	1970°C
5.	Density	1.898 kg/m <sup>3</sup> at 15°C
6.	Calorific value	47.1 MJ/kg
7.	Molecular weight	44.097 kg/k mole (propane) 58.12 kg/k mole (butane)
8.	Gaseous expansion	1L(liquid) = 0.27 m <sup>3</sup>
9.	Energy content	25 MJ/m <sup>3</sup>
10.	Chemical composition	$C_3H_8 + C_4H_{10}$
11.	Air/Fuel ratio	15.52 kg of air/kg of fuel

## OBJECTIVES

Literature review was taken up to work in the domain of flame tube. Based on the literature, the following objectives were formed.

- Replacing non-calibrated rotameters by calibrated ones & using pneumatic tubing to ensure leak proof flow of gases & analyzing the deviation in error.
- Partial automation of the setup using LDR sensors.
- Obtaining flame speed by using domestic LPG & calibrated LPG & analyzed the changes in flame speed.

## CHAPTER 4. EXPERIMENTAL SET-UP DESIGN FOR MEASURING FLAME SPEEDS



Fig. 4.1 Experimental setup

Table 4.1 List of components

List of components	Quantity
Flame tube	1
Flame arrester	1
Calibrated Rotameters	3
Buffer tank	1
Pneumatic Tubing	-
Ignition assembly (Lighter)	1
LPG Cylinder	1
Zero air cylinder	1
Calibrated LPG Cylinder	1
Pressure gauge	2
Wooden frame set-up	-

#### 4.1.1 FLAME TUBE



Fig. 4.2 Flame tube

A special polymer transparent tube of length 1m is used for flame propagation. Flame travels from one end of the tube to another end. One end of the tube acts as inlet for air-fuel mixture and other end is closed. Borosilicate glass is a type of glass with silica and boron trioxide as the main glass-forming constituents. Borosilicate glasses are known for having very low coefficients of thermal expansion ( $3 \times 10^{-6} K^{-1}$  at  $20^\circ C$ ), making them resistant to thermal shock, more so than any other common glass. Due to these properties of borosilicate glass we have used to conduct experiment on flame speed measurement. Such glass is less subject to thermal stress and is commonly used for the construction of reagent bottles.

### 4.1.2 FLAME ARRESTOR

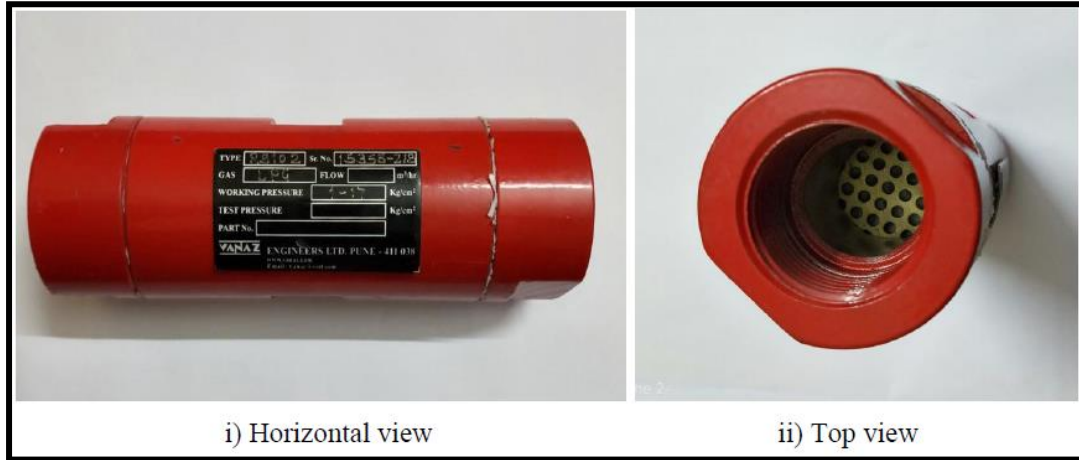


Fig.4.3 Flame arrestor

A flame arrestor is a device which allows gas to flow through it but stops the flame to prevent larger fire or explosion. It functions by absorbing the heat from a flame front travelling at particular velocities, thus drops the burning mixture below its auto-ignition temperature. Flame arresters have the same working principle: removing heat from the flame as it attempts to travel through narrow passages with walls of metal or other heat-conductive material.

### 4.1.3 CALIBRATED ROTAMETERS

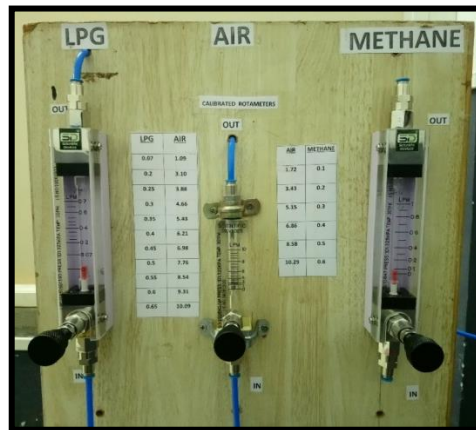


Fig. 4.4 Calibrated rotameters

Rotameter is a device that measures the volumetric flow rate of fluid in a closed tube. The range of the air rotameter used is 0-10 LPM and LPG rotameter is 0.07-0.7 LPM. A rotameter consists of a tapered tube, typically made of borosilicate glass with a 'float' (a shaped weight, made up of

PVC), inside that is pushed up by the drag force of the flow and pulled down by gravity. The drag force for a given fluid and float cross section is a function of flow speed squared only, as per drag equation.

A higher volumetric flow rate through a given area increases flow speed and drag force, so the float will be pushed upwards. However, as the inside of the rotameter is cone shaped (widens), the area around the float through which the medium flows increases, the flow speed and drag force decrease until there is mechanical equilibrium with the float's weight.

#### 4.1.4 BUFFER TANK



Fig. 4.5 Buffer tank

Buffer tank is used to maintain constant air flow through airline as there was change in cross section from  $d = 6.5\text{mm}$  (Rotameter outlet) to  $d = 25.4\text{mm}$  (Mixing chamber inlet). Air from rotameter enters the tank through a pipe of 6.5mm diameter. The buffer tank gets filled with air; air leaves the tank through a pipe of 25.4mm diameter. This maintains a constant mass flow rate across the airline.

#### 4.1.5 IGNITION ASSEMBLY



Fig. 4.6 Ignition assembly

It is used to ignite the air-fuel mixture. This authentic ignition chamber assembly is specially designed with the help of flame tube dimensions. It is attached directly to the other end of the flame tube. Igniter produces the spark to ignite the mixture. Here igniter used is lighter which is made up of plastic material and is inserted perpendicularly into the inline supply. When the lighter is ignited, the flame front travels from one end to the other end. The time is recorded for this process.

#### 4.1.6 PRESSURE REGULATOR



Fig. 4.7 Pressure regulator



A pressure gauge is a mechanical instrument designed to measure the internal and outlet pressure. A pressure regulator provides better resolution and control when its inlet and control range pressures closely match the pressure requirements of the fluid handling system. Here outlet pressure maintained for both air and fuel is 0.5 bar. This two-stage regulator is comparable to two single-stage regulators connected in series. The first stage shows inlet pressure. The second stage can be adjusted with the handle to achieve the required outlet pressure. This two-stage arrangement minimizes the supply-pressure effect caused by fluctuating inlet pressure, such as with a depleting gas cylinder. As inlet pressure drops below the setting of the first stage, the regulator then functions as a single-stage regulator. The first-stage pressure setting can be reduced while monitoring the pressure at the inter-stage port, but lower flow may result.

#### 4.1.7 DOMESTIC LPG CYLINDER



Fig. 4.8 Domestic LPG cylinder

Liquefied petroleum gas (LPG) is a portable, clean and efficient energy source which is readily available to consumers around the world. LPG is a co-product of natural gas and crude oil production; its unique properties make it versatile energy source which can be used in more than 1000 different applications. Liquefied Petroleum Gas (LPG) is made up of a combination of propane, butane, and trace amounts of other chemicals, including pentane. Butane comprises slightly less than 70 percent of the gas. Propane comprises nearly 29 percent of the gas, leaving just over 1 percent for the trace components.



#### 4.1.8 ZERO AIR CYLINDER



Fig. 4.9 Zero air cylinder

Zero air is an ambient air filtered to contain less than 0.1 parts per million (ppm) of total hydrocarbons. Zero Air is synthetic air provided by an expensive high-pressure gas cylinder. While this is a satisfactory method, the use of an in-house generator to provide Zero Air for FID detection is safer, more convenient, more reliable and more economical than the use of high pressure cylinders. An in-house Zero Air generator is completely automatic and requires a minimum of maintenance.

#### 4.1.9 CALIBRATED LPG CYLINDER



Fig.4.10 Calibrated LPG cylinders

Calibrated LPG is used to eliminate effect of different contaminants presents in domestic LPG on the calculation of the flame velocity. This Calibrated LPG is combination of 69.87% Propane and 30.13% n-Butane with higher purity.

#### 4.1.10 MIXING CHAMBER

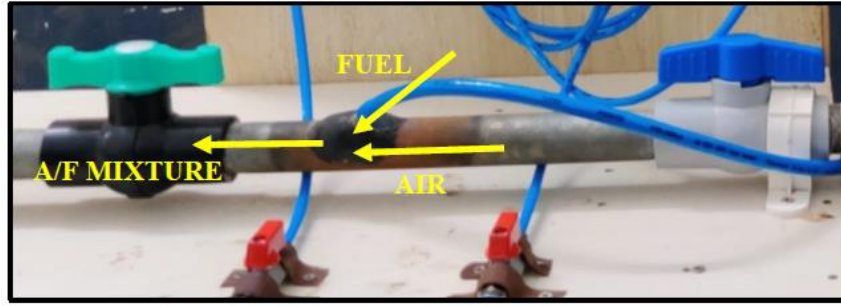
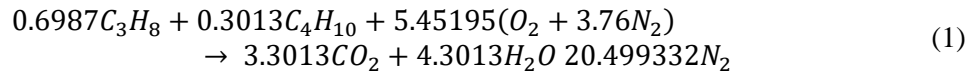


Fig. 4.11 Mixing chamber

Liquefied petroleum gas (LPG) was considered as a baseline fuel and dry air as an oxidizer. Based on stoichiometry (A/F) mass ratio of LPG – air mixture (15.52:1) and pipe diameter of 25.4 mm, a mixing chamber was designed. The principle followed was the area ratio matching with given A/F mass ratio.

For calibrated LPG (**69.87% by volume of Propane, 30.13% by volume of n-Butane**)



$$\left(\frac{A}{F}\right)_s = 15.52 \quad (2)$$

$$\frac{\text{Area of air port}}{\text{Area of fuel port}} = 15.52$$

#### 4.1.11 PNEUMATIC TUBING

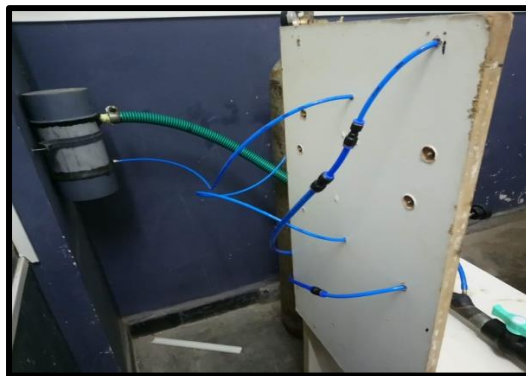


Fig. 4.12 Pneumatic tubing

Pneumatic tubing and hose is to convey pressurized air to actuators, valves, tools and other devices. The air supply and application set a base line for the necessary product performance. Flow requirement helps to determine hose or tubing size. Tubing is generally specified by outer diameter and wall thickness, while hose is specified by inner diameter regardless, choosing too small an inner diameter “chokes” flow and results in pressure losses, inefficiency and excessive fluid velocity that can shorten service life. Too large a diameter, on the other hand, results in higher than necessary weight, size and cost. Also ensure that products operate below the stated maximum working pressure.

#### **4.1.12 REDUCERS AND VALVES**

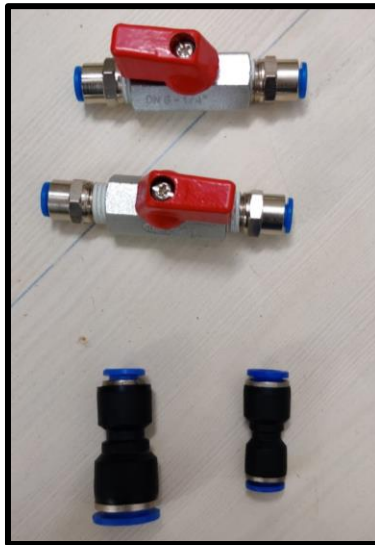


Fig. 4.13 Reducers and valves

A reducer is a kind of pipe fitting used in process piping that reduces the pipe size from a larger diameter to smaller diameter. A reducer allows for a change in pipe size to meet flow requirements of the system, reducer allows for a change in pipe size to meet hydraulic flow requirements of the system, or to adapt to existing piping of a different size. The length of the reduction is usually equal to the average of the larger and smaller pipe diameters.

A valve is a device that regulates, directs or controls the flow of a fluid by opening, closing, or partially obstructing various passageways. These valves are often used for routing process fluid to different locations, starting and stopping batch processes, and engaging automated safety (shutdown) functions.

#### 4.1.13 FIRE EXTINGUISHER



Fig. 4.14 Fire extinguisher

Fire extinguisher is a portable device that discharges a jet of water, foam, gas, or other material to extinguish a fire. A fire extinguisher is an active fire protection device used to extinguish or control small fires, often in emergency situations. It is not intended for use on an out-of-control fire, such as one which has reached the ceiling, endangers the user (i.e., no escape route, smoke, explosion hazard, etc.), or otherwise requires the expertise of a fire brigade. Typically, a fire extinguisher consists of a hand-held cylindrical pressure vessel containing an agent which can be discharged to extinguish a fire. Fire extinguishers manufactured with non-cylindrical pressure vessels also exist but are less common. As this experiment is based on usage of LPG and travelling of flame, one fire extinguisher is used to avoid critical/dangerous conditions.

## 4.2 MODIFICATION OF EXPERIMENTAL SETUP



Fig. 4.15 Fitting of calibrated rotameters

To maintain stable pressure in flame tube as well as to achieve more accuracy in measuring pressure of fuel and zero air, old rotameters are replaced with new calibrated rotameters. With these new calibrated rotameters, it is become easier to maintain stable and required pressure throughout the tube.

And hose pipes are replaced with pneumatic tubing along with different connectors and reducers to make the setup leakage proof, so that we can avoid leaking of fuel and air through different joints.

## CHAPTER 5: MEASUREMENT OF FLAME VELOCITY

### 5.1PROCEDURE TO MEASURE FLAME SPEED

- The gaseous fuel (LPG) and air are sent saperately into the mixing chamber and than sent at one end of the falme tube.
- The flow rates of the fuel and air are measured using rotameters.
- The fuel is ignited at the other end of the tube using a lighter.
- Flame velocity is measured as follows:
  - i. The air flow is switched off and the lighter is ignited at the same instant
  - ii. This is to make stagnation in the tube
  - iii. Stagnant air is essemstial for accurate measurement of flame velocity
  - iv. When the lighter is ignited, the flame front travels from one end to the other end. The time is recorded for this process.
  - v. The flame front terminates at the fuel supply end of the tube by a flame trap. (flame trap is made up of material with high specific heat)
  - vi. Thus by knowing distance travelled by flame and time, the flame velocity can be calculated.

## 5.2 COMPARING NON CALIBRATED ROTAMETERS READINGS WITH CALIBRATED ROTAMETRES READINGS

Table 5.1 Tabular column

**Readings (Non-calibrated Rota-meters):**

Sl. No.	Distance(m)	Time taken (T) sec.	Fuel flow (LPM)	Air flow (LPM)	Flame Velocity (m/sec)
1	2.3	3.90	0.05	7	0.58
2	2.3	3.84	0.05	7	0.59
3	2.3	4.10	0.05	7	0.56
4	2.3	3.77	0.05	7	0.60
5	2.3	4.45	0.05	7	0.50
<b>Average</b>					<b>0.566m/s</b>

**Readings (Calibrated Rota-meters)**

Sl. No.	Distance(m)	Time taken (T) sec.	Fuel flow (LPM)	Air flow (LPM)	Flame Velocity (m/sec)
1	2.3	4.08	0.10	5	0.560
2	2.3	4.64	0.07	5	0.495
3	2.3	4.65	0.07	5	0.494
4	2.3	4.68	0.07	5	0.490
5	2.3	3.92	0.09	5	0.580
<b>Average:</b>					<b>0.524m/s</b>

$$\text{Percentage Error} = \frac{\text{Average velocity with non calibrated rotameters} - \text{Average velocity with calibrated rotameters}}{\text{Average velocity with non calibrated rotameters}} \times 100$$

$$= \frac{0.566 - 0.524}{0.566} \times 100$$

$$\text{Percentage error} = 7.42\%$$

### 5.3 FLAME COLORS FOR DIFFERENT AIR FUEL RATIOS

LPG= full valve      AIR=0.5bar      Tube length=2.3m

Table 5.2 Flame color analysis

Sl. no.	Time taken(sec)	Fuel flow(LPM)	Air Flow(LPM)	Velocity(m/s)	Equivalence ratio ( $\phi$ )	color
1.	3.91	0.07	4	0.59	0.27	Blue
2.	4.08	0.10	5	0.56	0.31	Greenish blue
3.	4.64	0.07	5	0.495	0.217	Purple blue
4.	4.65	0.07	5.5	0.494	0.198	Purple
5.	4.70	0.10	6	0.49	0.258	Light purple
6.	4.65	0.07	5	0.494	0.217	Purple
7.	4.00	0.07	4.5	0.57	0.241	Blue
8.	4.68	0.07	5	0.49	0.217	Blue
9.	4.80	0.07	4.5	0.48	0.241	Blue
10.	3.92	0.09	5	0.58	0.279	Blue
11.	3.64	0.10	5.5	0.63	0.282	Greenish blue
12.	3.87	0.10	5.5	0.59	0.282	Blue
Avg. time =4.295 sec			Avg. velocity=0.538 m/s			

$$\text{Deviation from non-calibrated to calibrated rotameters} = \frac{0.566 - 0.538}{0.566}$$

$$\text{Percentage error} = 4.947\%$$



## CHAPTER 6: PARTIAL AUTOMATION OF EXPERIMENTAL SETUP

While taking time reading and calculating velocity of flame front, manual calculating using stopwatch leads to small error. To eliminate this minute error, this automated system with LDR (Light Dependent Resister) sensor is installed within the setup.

Components of automation system:

- Arduino UNO
- Two LDR sensors
- Wiring(Jumper Cables)
- LCD display

### 6.1 Arduino UNO

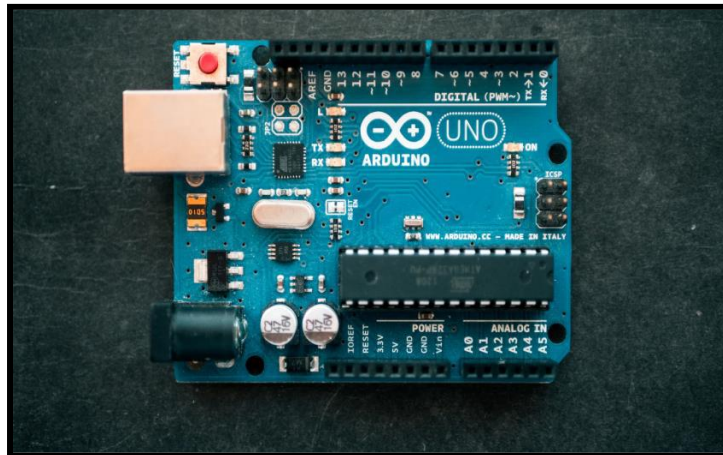


Fig. 6.1 Arduino board

Arduino is an open-source electronics platform based on easy-to-use hardware and software. Arduino boards are able to read inputs - light on a sensor and turn it into an output turning on an LED. We can instruct the board what to do by sending a set of instructions to the microcontroller on the board.

The LDR sensors were connected to Arduino and the board was programed in such a way that when first sensor senses the flame front timer will start automatically and will stop when the second sensor senses the flame front. The distance was predefined and the time and flame speed was displayed as output on the display.

## 6.2 LDR (Light Dependent Resistor) sensor

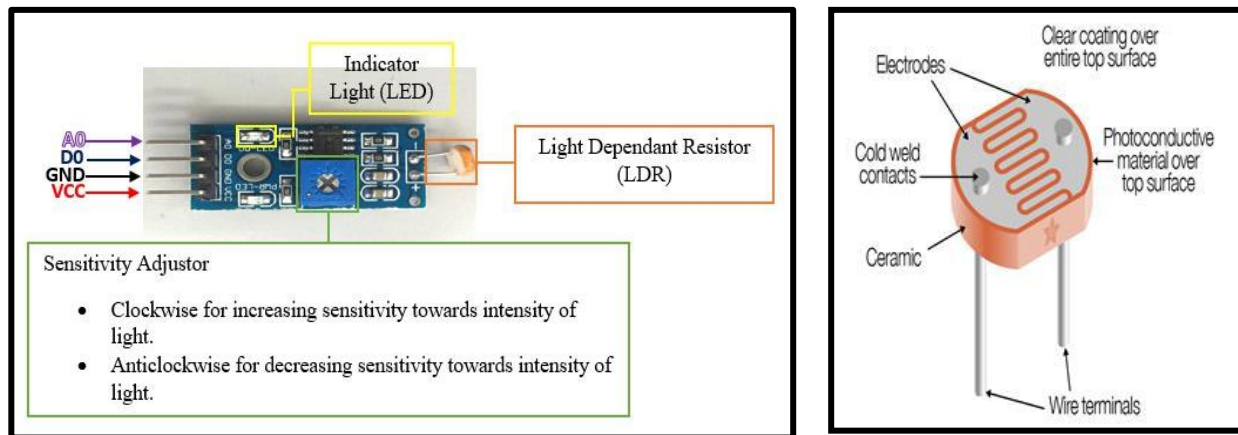


Fig.6.2 Detailed view of LDR sensor

LDR sensor is of two cadmium sulphide (cds) photoconductive cells with spectral responses similar to that of the human eye. The sensor that can be used to detect light is an LDR. Since the LDR gives out an analog voltage, it is connected to the analog input pin on the Arduino. The Arduino, with its built-in ADC (analog-to-digital converter), then converts the analog voltage. The photo-resistor, CdS, or LDR finds many uses as a low-cost photo sensitive element and was used for many years in photographic light meters as well as in other applications such as smoke, flame and burglar detectors, card readers and lighting controls for street lamps.

## 6.3 Wiring (Jump cable)

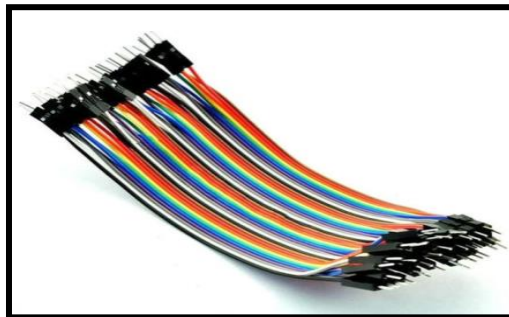


Fig.6.3 Jump cable

A jump wire is an electrical wire, or group of them in a cable, with a connector or pin at each end, which is normally used to interconnect the components of a breadboard or circuit, internally or with other equipment without soldering.

## 6.4 LCD Display



Fig.6.4 LCD Display

This 20x4 Character LCD Display is built-in with RW1063 controller IC which are 6800, 4 line SPI or I2C interface options. The WH2004G 20x4 LCD Display have the same AA size and pin assignment as existing WH2004A and WH2004B character LCD modules but with smaller outline and VA size.

This LCD has two registers, namely, Command and Data. Command register stores various commands given to the display. Data register stores data to be displayed. The process of controlling the display involves putting the data that form the image of what you want to display into the data registers, then putting instructions in the instruction register

## 6.5 PROGRAM DEVELOPED TO MEASURE THE FLAME VELOCITY

```
Const int ldr1 = 7;
const int ldr0 = 8;
double time1=0,time2=0,distance=2.3;
void setup() {
  Serial.begin(9600);
  pinMode(ldr1, INPUT);
  pinMode(ldr0, INPUT);
}

void loop() {
  if (!digitalRead(ldr0))
  {
    time1 = millis();
    while(1)
    {
      if(!digitalRead(ldr1))
      {
        time2 = millis();
        double t = (time2-time1)/1000;
        double v = distance/t;

        Serial.print("Time=");
        Serial.print(t);
        Serial.println(" sec");
        Serial.print("Velocity=");
        Serial.print(v);
        Serial.println(" m/s");
        break;
      }
    }
  }
}
```

## 6.6 PROCEDURE AFTER PARTIAL AUTOMATION

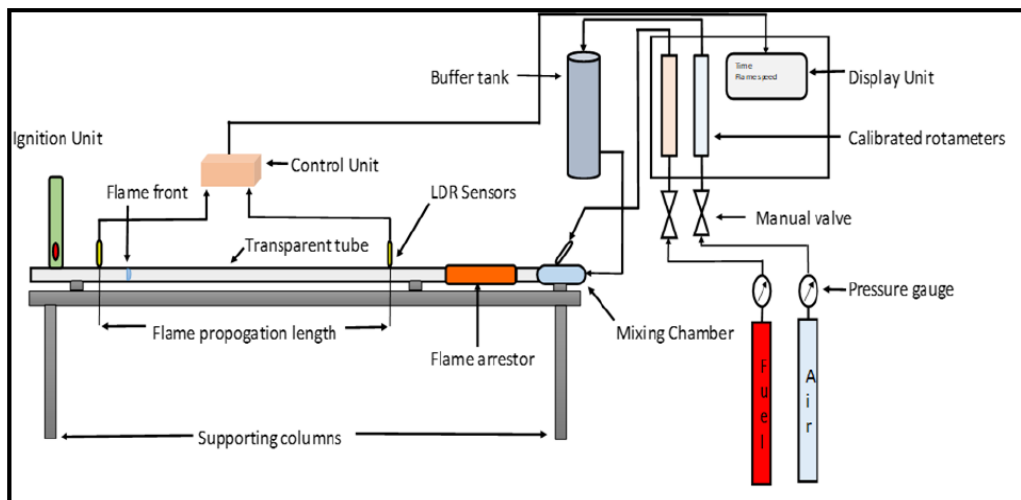


Fig. 6.5(a) Schematic of setup after automation

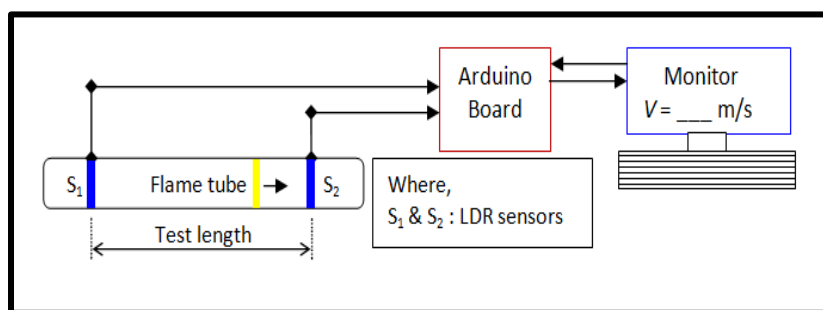


Fig. 6.5(b) Measurement chain system

The mixture of fuel and air was supplied to the mixing chamber. From operational point of view pressure factor emerging from domestic LPG cylinder and calibrated LPG cylinder was of utmost importance. The air cylinder was available with built-in pressure of 100 bar approximately, while domestic LPG and calibrated LPG was  $>2$  bar. Higher pressure of fuel cylinder was reduced and regulated by using a two-stage commercial regulator (output pressure = 1 bar) and air flow was also regulated with a two-stage air regulator (output pressure = 1 bar). Based on theoretical calculations, the fuel and air flow rates were set to operate the setup closer to stoichiometry condition. Calibrated rotameters (flow meters) were used to control the flow rates of LPG fuel and oxidizer as shown in Figure 3. The mixture of air and fuel was allowed to mix for some time before spark was triggered via ignition unit. Initiation of spark gave rise to a well-developed flame front propagating from left end to right end of the tube.

## CHAPTER 7: RESULTS AND DISCUSSION

Table 7.1 Comparison of manual readings with sensor readings

Readings with non-calibrated LPG

Air (LPM)	Fuel (LPM)	Sensor readings		Manual readings		Percentage error (%)	
		Time (sec)	Velocity (m/s)	Time (sec)	Velocity (m/s)	Time	Velocity
4.5	0.07	4.20	0.5476	4.39	0.52	4.52	5.04
4.5	0.07	3.38	0.6005	3.93	0.58	2.61	3.4
4.38	0.07	3.32	0.6928	3.40	0.6765	2.41	2.35
4.3	0.07	4.08	0.5637	4.14	0.55	1.44	2.43
4.3	0.07	3.57	0.65	3.60	0.6388	2.5	1.72
<b>Average</b>		<b>3.71sec</b>	<b>0.61m/s</b>	<b>3.892sec</b>	<b>0.593m/s</b>		

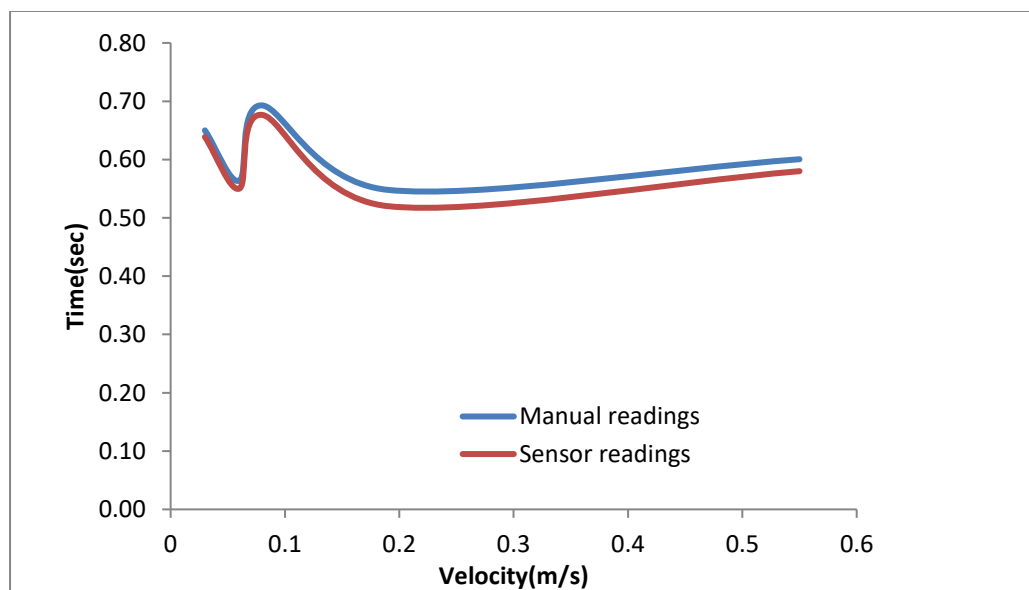


Fig. 7.1 Time V/s velocity plot

Experiments at ambient conditions (303 K & 101.325 kPa) were conducted to measure flame speeds on an in-house developed flame tube apparatus. By conducting experimentation with automated system i.e. using sensors reported readings which are close to that of manual readings. Fig.7.1 shows time V/s velocity plot, from which we come to know that there is not much deviation but automated system will provide us more accurate results than that of the manual method.

Table 7.2 Laminar flame speed for LPG-Air mixture

Fuel	Oxidizer	Manually recorded		Sensor recorded		% error w.r.t. flame speed
		Time (sec)	Flame speed (m/s)	Time (sec)	Flame speed (m/s)	
Indian domestic LPG fuel	Air	3.48	0.575	3.43	0.583	1.37
		3.44	0.581	3.38	0.591	1.69
		3.40	0.588	3.36	0.595	1.17
Calibrated LPG fuel	Air	4.14	0.483	4.10	0.487	0.82
		3.61	0.554	3.59	0.557	0.54
		3.76	0.531	3.71	0.539	1.48

The outcome of experiments with domestic and calibrated LPG – air mixtures is set out in Table 7.2. The average time interval of flame propagation and the average laminar flame speed with domestic LPG air mixture on manual mode was 3.44 sec & 0.58 m/sec respectively. Whereas, the sensor based obtained values stood at 3.39 sec & 0.59 m/sec respectively. The error in flame speed measurement is within 2%.

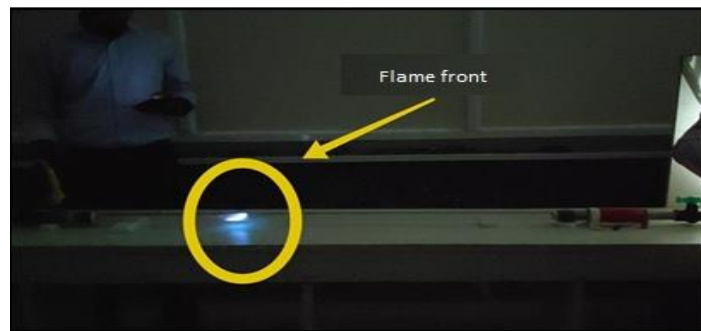


Fig.7.2 Propagation of flame front

The customized calibrated LPG (69.87% propane and 30.13% n-butane) – air mixtures under manual mode measurement resulted in 3.83 sec and 0.52 m/sec respectively. Whereas, the electronic based measurement recorded 3.80 sec & 0.53 m/sec respectively. A similar type of work was reported by Ajay et al., 2018 with customized LPG fuel (n-butane: 44.98%, propane 39.9%, methane: 1.9%, ethane: 4.1% and pentane: 9.12%). Flame speed of 0.55 m/sec at  $\phi = 1$  & 0.57 m/sec at  $\phi = 1.2$  was obtained with burner method. On comparison, the flame speeds on present work with lean mixtures is close and the deviation is attributed to variation in LPG fuel content and method followed.

Furthermore, distorted flame shapes were observed at extreme limits of lean or fuel rich conditions. The possible cause may be attributed to viscous and wall quenching effects. One such elongated higher amplitude flame front curvature in suspended form at fuel rich condition is shown in Fig.7.2. The flame colors were also quite different with domestic and standard calibrated LPG fuels as shown in Fig.7.3 & Fig.7.4.



Fig.7.3 Domestic LPG flame front



Fig.7.4 Calibrated LPG flame front



**CHAPTER 8: PROJECT EXPENDITURE**

Table 8.1 Project Expenditure

SL. NO.	COMPONENT	PROVIDER	QUANTITY	PRICE PER UNIT	TOTAL
1	CALIBRATED RORAMETERS	SCIENTIFIC DEVICES PVT. LTD.	3	4268	8536/-
2	PRESSURE REGULATOR	SANGHANI AGENCIES	1	4279/-	4279/-
3	PNEUMATIC PIPES	SUYASH HYDROPNEUMATICS	1m	163/-	163/-
4	ZERO AIR CYLINDER DEPOSIT	SHRI VENKATESH ENTERPRISES		7000/-	7000/-
5	METHANE GAS	SANGHANI AGENCIES	1	17700/-	17700/-
6	CALIBRATED LPG	SANGHANI AGENCIES	1	17700/-	17700/-
7	MINI BALL VALVE	VED CONTROLS	2	150/-	300/-
8	MALE CONNECTOR	VED CONTROLS	4	28/-	112/-
9	REDUCERS	SUYASH HYDROPNEUMATICS	6		350/-
10	ZERO AIR CYLINDER RE-FILL	SHRI VENKATESH ENTERPRISES	3	1652/-	4956/-
11	DOMESTIC LPG		1	800/-	800/-
12	TRANSPORTATION				1000/-
13	MISCELLANEOUS CHARGES				2000/-
14	PNEUMATIC PIPE	APG AUTOMOBILE PVT. LTD.	6m	48/-	288/-
15	PUSH IN CONNECTORS	APG AUTOMOBILE PVT. LTD.	6	164/-	984/-
16	ARDUINO BOARD		1	500	
17	LDR SENSOR		2	147	
18	DISPLAY	AMAZON	1	339	
<b>GRAND TOTAL</b>					<b>67,301/-</b>

## CHAPTER 9: GANTT CHART

Table.9.1 Gantt chart

Month/ Task	A U G	S E P T	O C T	N O V	D E C	J A N	F E B	M A R	A P R
Planning									
Literature									
Project mapping									
Cost estimation									
Testing									
Modification									
Trials/ Tabulation									
Report work									
Procurement of zero air & regulator									
Automation of setup									
Testing with domestic LPG									
Testing with calibrated LPG									
Final report									

## CHAPTER 10: SCOPE AND CONCLUSION

### SCOPE:

- Improved ignition unit which can generate a high voltage spark has to be setup which might be one of the reasons for not getting flame at stoichiometry.
- Mixing chamber can be modified by giving multiple fuel inlets radially or introduction of baffle plates so that proper mixing can occur.
- At stoichiometry condition in the present work, an issue of triggering was encountered, may be because of insufficient voltage at the electrode terminals.
- Furthermore, distorted flame shapes at extreme flammable limits (lean or fuel rich conditions) were observed. The possible cause may be because of viscous and wall quenching effects.

### CONCLUSION:

Average flame speeds for three different fuels were experimentally measured by improvising the setup and operating the setup closer to stoichiometry.

Fuels	Flame speed (m/s) (experimentally obtained)	Flame speed (m/s) (literature reported)
Domestic- LPG	0.59	0.575
Calibrated- LPG	0.53	0.575





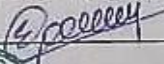

To overcome manual errors in measurement of flame propagation time interval (and therefore flame speeds), a multidisciplinary approach (with a mix of combustion science, electronics and coding interface) was followed. Under premixed and ambient conditions, the average laminar flame velocity of domestic LPG and calibrated LPG was found to be 0.59 m/sec & 0.53 m/sec respectively at lean condition. The error in manual measurement of flame velocities were well within 2%. The measurement of flame velocity finds its place in burn rate modeling studies, and it is a part of future work.

## REFERENCES

- D.P. MISHRA, “Fundamentals of Combustion”, department of Aerospace Engineering, IIT Kanpur, India.
- V GANESAN, “Internal Combustion Engines”, department of Mechanical Engineering, IIT Madras, Chennai, India. 3<sup>rd</sup> edition.
- Taylor, Simon Crispin (1991) Burning velocity and the influence of flame stretch unpublished Ph.D. thesis, Department of Fuel and Energy University of Leeds, UK.
- Noor M, Wandel AP, Yusaf T. Effect of air-fuel ratio on temperature distribution and pollutants for biogas MILD combustion. International Journal of Automotive and Mechanical Engineering. 2014;10:1980-92.
- Bosschaart KJ, De Goeij L. The laminar burning velocity of flames propagating in mixtures of hydrocarbons and air measured with the heat flux method. Combustion and Flame. 2004;136:261-9.
- Hu E, Huang Z, He J, Jin C, Zheng J. Experimental and numerical study on laminar burning characteristics of premixed methane–hydrogen–air flames. International Journal of Hydrogen Energy. 2009;34:4876-88.
- Kochar. Y TL, J. Seitzman. Laminar Flame Speeds of C1-C3 Alkanes at Elevated Pressure and Temperature with Dilution. presented at the Proceedings of the 6th US National Combustion Meeting. 2009.
- Yu Cheng CT, Zuohua Huang. Kinetic analysis of H<sub>2</sub> addition effect on the laminar flame parameters of the C1-C4 n-alkane-air mixtures: From one step overall assumption to detailed reaction mechanism. International Journal of Hydrogen Energy. 2015;40:703-18.
- D.P. Mishra, “Fundamentals of combustion,” Prentice-Hall of India publications, New Delhi, 2008. pp.6-7
- Ajay Tripathi, H.Chandra and M.Agarwal. Effect of mixture constituents on the laminar burning velocity of LPG-CO<sub>2</sub>-Air mixtures, ARPN Journal of Engineering and applied Sciences. Vol 2, NO.3, March 2010.
- I. Glassman, “Combustion”, Academic Press, USA, 4<sup>th</sup> Edition, 2008. Pg.714.





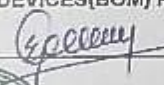

## APPENDIX

## Test and Calibration Report for Air Rotameter


 <b>Scientific Devices</b> (Bombay) Pvt. Ltd. An ISO9001-2015 Company		  	
Office No. 53, Shree Manoshi Complex, Plot No. 5 & 6, Sector 3, Opp. Ghansoli Railway Station, Ghansoli (E), Navi Mumbai - 400701, Maharashtra, INDIA. Tel. : +91-2549 1407, 2549 1408, 2549 1409, 2549 2779, 2549 2780, 2535 5092, 2535 3530, 2535 3505 Email : sdbpl@vsnl.com / sales@scientificdevices.org Web : www.scientificdevices.org			
<b>TEST &amp; CALIBRATION REPORT</b>			
REF. NO. : SDBPL/TR1/1900627/2019-2020	P.O. NO. : JCE/GEN/2019-20/097	DATE : 06/06/2019	
DATE : 26/06/2019	W.O. NO. : 1900627	DATE : 06/08/2019	
CLIENT : M/S. JAIN COLLEGE OF ENGINEERING			
ITEM : ACRYLIC BODY ROTAMETER WITH VERTICAL SCREWED CONNECTION AND WITH ISOLATION VALVE		IS NO. : 19061302	
QTY. : 1 NO.		TAG NO. : 1 PRODUCT CODE : SDASIV	
<b>OPERATING CONDITIONS :</b>		<b>MATERIAL :</b>	
FLUID/OPT.DENSITY/OPT.VI SCOSITY/OPT.TEMP/OPT.PRESSURE :		METERING TUBE : SOLID TRANSPARENT ACRYLIC	
AIR/1 2928 KG-M3/0.017 CP/301 DEG K/101.325 KPA		FLOAT : SS316	
FLOW RANGE : 1 - 10 LPM		GLAND PACKING : NEOPRENE	
STATE : GAS		END FITTING/FLANGE : SS304	
		SCALE : BLACK ANODIZED	
		W.E. : 13.82	
<b>PHYSICAL DETAILS :</b>		<b>SIZE&amp;CONNECTION</b>	
F/F OR C/C DISTANCE : 160 MM		1/4"BSP(M)	
MODELING/DESIGN PRESS : SDA-10/ 5KG/CM2		DIRECTION OF FLOW : VERTICAL	
<b>TEST CONDUCTED :</b>		<b>OBSERVATION</b>	
DIMENSIONAL CHECK : OK		± 2MM	
HYDRO TEST : 7 KG/CM2		NO LEAK	
REMARKS : Above instruments has been tested by calibrated pressure guage bearing Sr.no. 5364-O and its Recalibration due on 23/08/2019.		REMARKS : ACCEPTABLE ACCEPTABLE	
<b>CALIBRATION REPORT :</b>			
S.R.NO	ROTAMETER READING IN LPM	WATER EQUIVALENT IN LPM	ACTUAL FLOW IN LPM
			TAG NO. : IS.N 19061302
1)	10	0.230	0.232
2)	8	0.184	0.186
3)	6	0.138	0.140
4)	4	0.092	0.093
5)	2	0.046	0.047
6)	1	0.023	0.023
REMARKS : A) Accuracy within ±2% of FSD B) Calibration method confirms to ISA R.P.16.6 C) Master reference system calibrated by weight & measure department having traceability no.9120180911547. D) This certificate is valid for a period of 12 months from the date of calibration.			
For SCIENTIFIC DEVICES (BOM) PVT. LTD.			
SIGN. 		DATE :	
			






## Test and Calibration Report for Methane Rotameter

 <b>Scientific Devices</b> (Bombay) Pvt. Ltd. An ISO9001-2015 Company		  	
Office No. 53, Shree Manoshi Complex, Plot No. 5 & 6, Sector 3, Opp. Ghansoli Railway Station, Ghansoli (E), Navi Mumbai - 400701, Maharashtra, INDIA. Tel. : +91-2549 1407, 2549 1408, 2549 1409, 2549 2779, 2549 2780, 2535 5092, 2535 3530, 2535 3505 Email : sdbpl@vsnl.com / sales@scientificdevices.org Web : www.scientificdevices.org			
<b>TEST &amp; CALIBRATION REPORT</b>			
REF. NO.: SDBPL/TR1/1900627/2019-2020		P.O.NO.: JCE/GEN/2019-20/097	DATE: 06/06/2019
DATE: 26/06/2019		W.O.NO.: 1900627	DATE: 06/08/2019
CLIENT: M/S. JAIN COLLEGE OF ENGINEERING			
ITEM: PURGE ROTAMETER WITH VERTICAL SCREWED CONNECTION AND WITH ISOLATION VALVE		IS NO: 19061304	
QTY: 1 NO.		TAG NO: 3 PRODUCT CODE: STVSV	
<b>OPERATING CONDITIONS:</b>		<b>MATERIAL:</b>	
FLUID/OPT.DENSITY/OPT. VISCOSITY/OPT. TEMP/OP T.PRESSURE :	METHANE/0.647 KG/M3/0.017 CP/301 DEG K/101.325 KPA	METERING TUBE	BOROSILICATE GLASS
		FLOAT	PVC
		WETTED PARTS/END FITTING	SS304 & SS304
		GLAND PACKING	NEOPRENE
		SCALE	ENGRAVED
		WE	0.46
FLOW RANGE:	0.1 - 1 LPM		
STATE:	GAS		
<b>PHYSICAL DETAILS:</b>		<b>SIZE&amp;CONNECTION</b>	
F/F OR C/C DISTANCE:	250 MM	SIZE&CONNECTION	1/4"BSP(M)
MODELNO/DESIGN PRESS:	ST-4/5 KG/CM2	DIRECTION OF FLOW	VERTICAL
<b>TEST CONDUCTED:</b>		<b>OBSERVATION</b>	
DIMENSIONAL CHECK: OK		± 2MM	
AIRLEAK TEST: KG/CM <sup>3</sup>		NO LEAK	
HYDRO TEST: KG/CM <sup>3</sup>		NO LEAK	
REMARKS: Above instruments has been tested by calibrated pressure guage bearing Sr.no. 5364-O and its Recalibration due on 23/08/2019.		ACCEPTABLE	
<b>CALIBRATION REPORT:</b>			
S.R.NO.	ROTAMETER READING IN LPM	WATER EQUIVALENT IN LPM	ACTUAL FLOW IN LPM
			TAG NO.: IS.N.19061304
1)	1	0.008	0.008
3)	0.8	0.006	0.006
5)	0.6	0.005	0.005
7)	0.4	0.003	0.003
9)	0.2	0.002	0.002
10)	0.1	0.001	0.001
REMARKS: A) Accuracy within ±2% of FSD B) Calibration method confirms to ISA R.P.15.6 C) Above flowmeter has been calibrated by Borosil standard calibrated jar Class 'A' certified. D) This certificate is valid for a period of 12 month from the date of calibration.			
For SCIENTIFIC DEVICES(BOM) PVT. LTD.			
SIGN. 		DATE:	
			



## Test and Calibration Report for LPG Rotameter



**Scientific Devices**  
(Bombay) Pvt. Ltd.  
— An ISO9001-2015 Company —

Office No. 53, Shree Manoshi Complex, Plot No. 5 & 6, Sector 3,  
Opp. Ghansoli Railway Station, Ghansoli (E), Navi Mumbai - 400701,  
Maharashtra, INDIA. Tel. : +91-2549 1407, 2549 1408, 2549 1409, 2549 2779,  
2549 2780, 2535 5092, 2535 3530, 2535 3505  
Email : sdbpl@vsnl.com / sales@scientificdevices.org  
Web : www.scientificdevices.org

**TEST & CALIBRATION REPORT**

REF. NO. : SDBPL/TR1/1900627/2019-2020	P.O.NO. : JCE/GEN/2019-20/097	DATE. : 06/06/2019
DATE : 26/06/2019	W.O.NO. : 1900627	DATE. : 06/08/2019
CLIENT : M/S. JAIN COLLEGE OF ENGINEERING		

ITEM : PURGE ROTAMETER WITH VERTICAL SCREWED CONNECTION AND WITH ISOLATION VALVE	IS NO. : 19061303  TAG NO. : 2 PRODUCT CODE : STVSV
QTY. : 1 NO.	

OPERATING CONDITIONS :		MATERIAL :	
FLUID/OPT.DENSITY/OPT. VISCOSITY/OPT.TEMP/OP T.PRESSURE =	LPG (GAS)/1.95 KG/M3/0.017 CP/301 DEG K/101.325 KPA	METERING TUBE :	BOROSILICATE GLASS
		WETTED PARTS/END FITTING :	SS304 & SS304
FLOW RANGE :	0.07 - 0.7 LPM	GLAND PACKING :	NEOPRENE
STATE :	GAS	SCALE :	ENGRAVED
		W.E. :	0.55

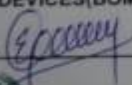
PHYSICAL DETAILS :		OBSERVATION	
F/F OR C/C DISTANCE :	250 MM	SIZE&CONNECTION :	1/4"BSP(M)
MODELNO/DESIGN PRESS :	ST-4/5 KG/CM2	DIRECTION OF FLOW :	VERTICAL


TEST CONDUCTED :		OBSERVATION		REMARKS	
DIMENSIONAL CHECK :	OK	± 2MM	ACCEPTABLE	ACCEPTABLE	ACCEPTABLE
AIRLEAK TEST :	3 KG/CM²	NO LEAK			
HYDRO TEST :					
REMARKS : Above instruments has been tested by calibrated pressure guage bearing Sr.no. 5364-D and its Recalibration due on 23/08/2019.					

CALIBRATION REPORT :							
S.R.NO.	ROTAMETER READING IN LPM	WATER EQUIVALENT IN LPM	ACTUAL FLOW IN LPM				
			TAG NO. :				
			IS N 19061303				
1)	0.7	0.009	0.009				
2)	0.6	0.008	0.008				
4)	0.4	0.005	0.005				
6)	0.2	0.003	0.003				
8)	0.07	0.001	0.001				


REMARKS : A) Accuracy within ±2% of FSD  
B) Calibration method confirms to ISA R.P.16.6  
C) Above flowmeter has been calibrated by Borosil standard calibrated jar Class 'A' certified.  
D) This certificate is valid for a period of 12 month from the date of calibration.

For SCIENTIFIC DEVICES(BOM) PVT. LTD.

SIGN.  DATE :



## Concentration Report of Calibrated LPG



## SANGHANI AGENCIES

DISTRIBUTORS IN:

✧ AMMONIA GAS ✧ NITROGEN ✧ OXYGEN ✧ ARGON ✧ FREEZOL-68-OIL  
✧ CARBON DIOXIDE ✧ LIQUOR AMMONIA ✧ DISSLOVED ACETYLENE ✧ SF6 ✧ HYDROGEN  
✧ HELIUM ✧ FRAYON ✧ CALIBRATION GASES & ALL OTHER MIXTURE GASES

86/1, Dhauji - Old Goa, Goa 403 402. Ph.: 2285775, 2285373, 2285774  
Fax No.: (0832) 2285373 Mobile : 9822123715  
Email : sanghanigas@yahoo.co.in

---


To,  
Jain College of Engineering,  
599/2, T.S. Nagar,  
Hunchanhatti Cross Machhe,  
Belgavi-590014,  
Karnataka.

**TO WHOMSOEVER IT MAY CONCERN**

We hereby confirm that 01 No. of CLAIBRATION Gas Cylinder Supplied vide our  
Challan No: 3989 Dt: 05/09/2019 are as per below specification.

COMPONENT NAME	REQUIRED CONCENTRATION	ACTUAL CONCENTRATION
PROPANE	70%	69.87%
N-BUTANE	30%	30.13%

CYL.NO. 72219



For SANGHANI AGENCIES  
Analyst

Any Dispute subject to Goa Jurisdiction only